EARTHQUAKE SIMULATION TESTS OF A LOW-RISE METAL STRUCTURE

by

J.S. Hwang, K.C. Chang, G.C. Lee and R.L. Ketter

Department of Civil Engineering
State University of New York at Buffalo
Buffalo, NY 14260

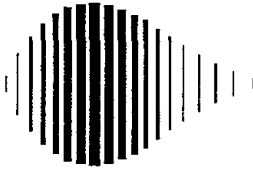Technical Report NCEER-88-0026

August 1, 1988

NOTICE

This report was prepared by the State University of New York at Buffalo as a result of research sponsored by the National Center for Earthquake Engineering Research (NCEER) and the National Science Foundation. Neither NCEER, associates of NCEER, its sponsors, State University of New York at Buffalo, nor any person acting on their behalf:

a. makes any warranty, express or implied, with respect to the use of any information, apparatus, method, or process disclosed in this report or that such use may not infringe upon privately owned rights; or

b. assumes any liabilities of whatsoever kind with respect to the use of, or for damages resulting from the use of, any information, apparatus, method or process disclosed in this report.

I.a

EARTHQUAKE SIMULATION TESTS OF
A LOW-RISE METAL STRUCTURE

by

J.S. Hwang[1], K.C. Chang[2], G.C. Lee[3] and R.L. Ketter[4]

August 1, 1988

Technical Report NCEER-88-0026

1   Research Associate, Dept. of Civil Engineering, State University of New York at Buffalo
2   Research Assistant Professor, Dept. of Civil Engineering, State University of New York at Buffalo
3   Professor and Dean of Engineering, Dept. of Civil Engineering, State University of New York at Buffalo
4   Professor of Civil Engineering, and Director, NCEER, State University of New York at Buffalo
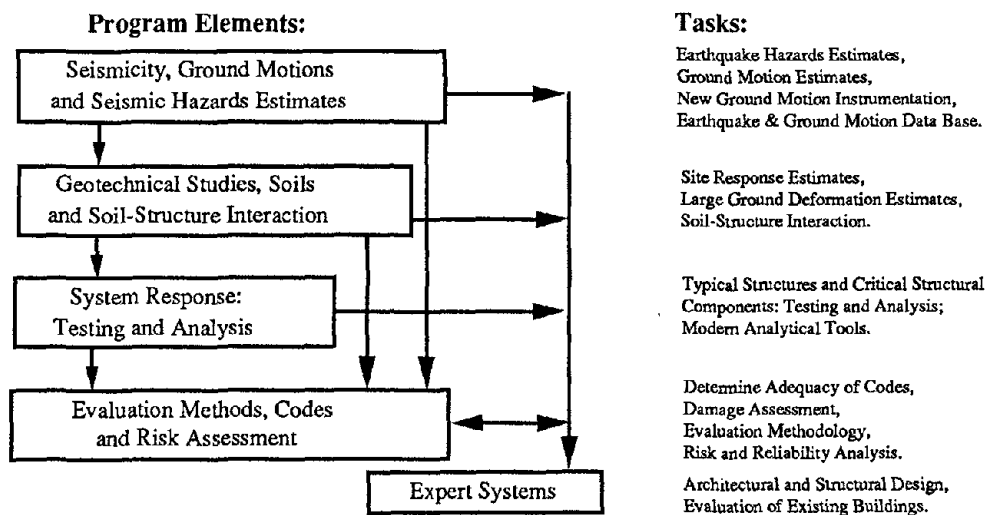
PREFACE

The National Center for Earthquake Engineering Research (NCEER) is devoted to the expansion of knowledge about earthquakes, the improvement of earthquake-resistant design, and the implementation of seismic hazard mitigation procedures to minimize loss of lives and property. Initially, the emphasis is on structures and lifelines of the types that would be found in zones of moderate seismicity, such as the eastern and central United States.

NCEER's research is being carried out in an integrated and coordinated manner following a structured program. The current research program comprises four main areas:

- Existing and New Structures
- Secondary and Protective Systems
- Lifeline Systems
- Disaster Research and Planning

This technical report pertains to Program 1, Existing and New Structures, and more specifically to System Response.

The long term goal of research in Existing and New Structures is to develop methods for rational probabilistic risk assessment for damage or collapse of structures, mainly existing buildings, especially in regions of moderate seismicity. The work will rely on improved definitions of seismicity and site response, experimental and analytical evaluations of systems response, and more accurate assessment of risk factors. This technology will be incorporated in expert systems tools and improved code formats for existing and new structures. Methods of retrofit will also be developed. When this work is completed, it should be possible to characterize and quantify societal impact of seismic risk in various geographical regions and large municipalities. Toward this goal, the program has been divided into five components, as shown in the figure below:

Program Elements:

Seismicity, Ground Motions and Seismic Hazards Estimates
Geotechnical Studies, Soils and Soil-Structure Interaction
System Response: Testing and Analysis
Evaluation Methods, Codes and Risk Assessment
Expert Systems

Tasks:

Earthquake Hazards Estimates,
Ground Motion Estimates,
New Ground Motion Instrumentation,
Earthquake & Ground Motion Data Base.

Site Response Estimates,
Large Ground Deformation Estimates,
Soil-Structure Interaction.

Typical Structures and Critical Structural Components: Testing and Analysis;
Modern Analytical Tools.

Determine Adequacy of Codes,
Damage Assessment,
Evaluation Methodology,
Risk and Reliability Analysis.

Architectural and Structural Design,
Evaluation of Existing Buildings.

System Response Studies constitute one of the important areas of research in Existing and New Structures. Current research activities include the following:

1. Testing and analysis of lightly reinforced concrete structures, and other structural components common in the eastern United States such as semi-rigid connections and flexible diaphragms.
2. Development of modern, dynamic analysis tools.
3. Investigation of innovative computing techniques that include the use of interactive computer graphics, advanced engineering workstations and supercomputing.

The ultimate goal of projects concerned with System Response Studies is to provide an estimate of the seismic hazard of existing buildings which were not designed for earthquakes and to provide information on typical weak structural systems, such as lightly reinforced concrete elements and steel frames with semi-rigid connections. An additional goal of these projects is the development of modern analytical tools for the nonlinear dynamic analysis of complex structures.

One of the major problems that currently exists with regard to seismic analysis and design of gable framed metal structures is the lack of reliable laboratory tests. This study is concerned with providing that type of information. A typically proportioned gable frame was designed using the current AISC specification, and that structure was tested on the shaking table to ascertain its performance under a variety of seismic excitations. One interesting and important observation was that the "R" factor now contained in most earthquake codes is considerably at variance with laboratory observed values - by a factor of one-half or more.

Retrofit of metal gable frame structures also is of concern, and this investigation examines one particular type of such strengthening.

ABSTRACT

In the United States, design of steel gable frames normally follows the guide-
lines of the American Institute of Steel Construction for assumed wind and gravity
loads. In this study, a pinned-base steel gable frame structure composed of pris-
matic members was so designed, and its seismic behavior was investigated using
the shaking table. The structure was tested well into the inelastic range so that
its ultimate lateral strength could be evaluated and quantified. It was observed
that pinned-base steel gable frames designed according to the AISC specifications
under normal gravity and wind loads would not perform satisfactorily under strong
earthquake ground motions when measured by the limitations specified by UBC
and ATC.

The feasibility and efficiency of structural retrofit also was observed for one type
of knee brace. This initial investigation suggests that much subsequent strength and
ductility can be achieved for the type of structure studied.

TABLE OF CONTENTS

LIST OF ILLUSTRATIONS

LIST OF ILLUSTRATIONS (Cont'd)

LIST OF TABLES

TABLE	TITLE	PAGE

xi

SECTION 1

INTRODUCTION

Steel gable frames with and without tapered members have been widely used throughout the world over the past 30 to 50 years. In the United States, the design of these structures normally assumes that the gravity and wind loads are static loadings, and that the members are proportioned based on the AISC Specifications [1,2].

Studies of the inelastic behavior and ultimate strength of structural members, subassemblages and frames have been extensive during the last two decades. However, these efforts have been mainly devoted to regular shear type buildings. Little attention has been paid to the inelastic behavior of irregular structures such as steel gable frames subjected to seismic loading. In the literature there are only a limited number of documents, and those describe the cyclic inelastic behavior of subassemblages of steel gable frame composed of prismatic members[3]. For tapered members, none has been found.

In design practice, both allowable stress design and plastic design are applicable for steel gable frames composed of prismatic members. For gable frames composed of tapered members, only allowable stress design is permitted by the AISC Specifications [1,4]. Very limited information is readily available for the design of steel gable frames subjected to strong earthquake ground motions.

The purpose of this study, therefore, is to investigate experimentally, using a shaking table, the general seismic behavior of a pinned-base steel gable frame composed of prismatic members. Test results are compared with current seismic design

practice [5,6], and important design parameters warranting special consideration by design engineers are summarized.

SECTION 2
TEST STRUCTURE

Because many steel gable frames composed of prismatic members have been designed and fabricated, and most of these have assumed a pinned-base condition, a symmetric steel gable frame with pinned-bases and prismatic members was used for this study. The complete test set-up consisted of two parallel frames, two concrete blocks (or loading masses) mounted on a supporting frame between the two test frames, and a foundation (see Fig. 2–1). The supporting frame was attached to the two planar test frames by simple connections. The foundation was composed of a steel skeleton and two concrete beams, which were attached to the shaking table. The dimensions of the test structure are given in Fig. 2–2.

In order to avoid the necessity for special fabrication of a small-scaled section, which would have been required by strict application of modeling laws [10,11], the smallest rolled section, W6x9, was used for both the rafters and the columns of the test structure. The panel zones of the column–to–rafter connections were stiffened by two doubler-plates to avoid the formation of plastic hinges within the panel zones. The test structure was assumed to be a typical gable frame, but not necessarily a scaled model of any particular prototype. The details of the structural configuration and the instrumentation were reported in Ref. [8].

The total weight of the roofing system, which included two concrete blocks, each weighing 3.5 kips, and their supporting frame, was about 4 kips on each test frame. Structurally, each frame was subjected to three concentrated vertical loads at the location of three interconnecting or cross beams, W6x12. The three concentrated
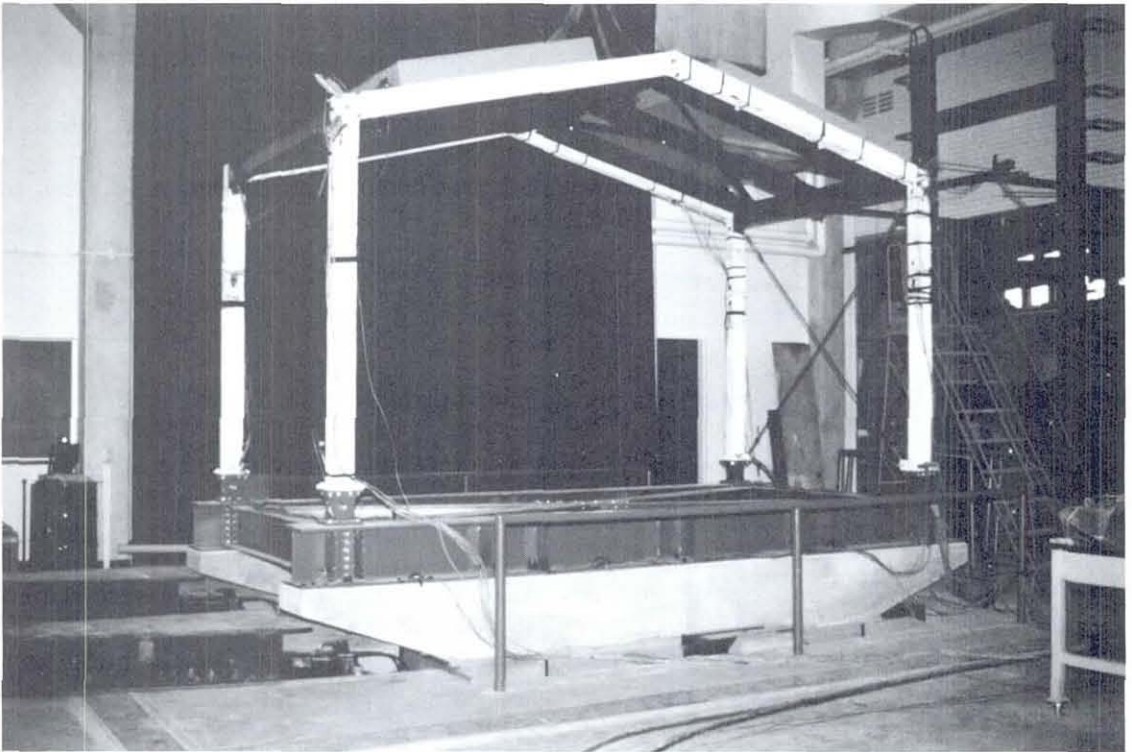
FIGURE 2-1 Photograph of Test Structure
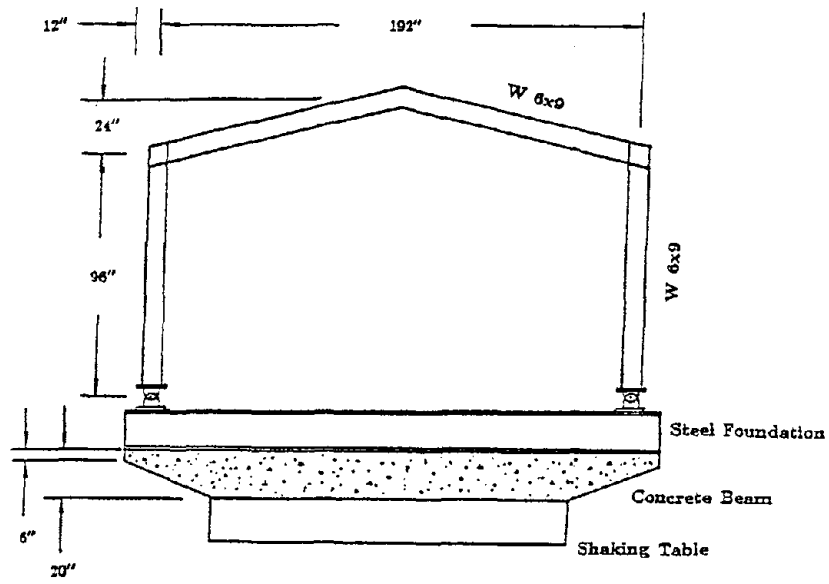
Front View of Test Set Up
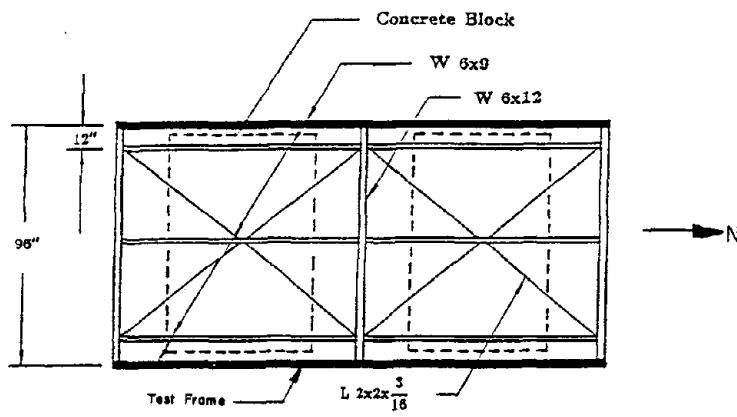
Top View of Test Structure
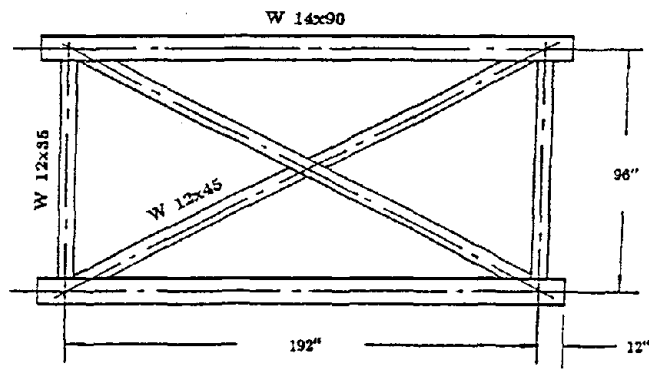
Top View of Steel Foundation

FIGURE 2-2 Dimensions of Test Structure

2-3

loads caused a static in-plane bending moment diagram which was different from that which could correspond to a uniformly distributed load. This gravity load was employed to simulate the lumped masses which were seismically effective, rather than structurally effective. The design check according to AISC formulas showed that the test frame was over-designed. The combined stress ratios are shown in Fig. 2-3. As can be realized from this figure, the test frame possesses a strong lateral capability.
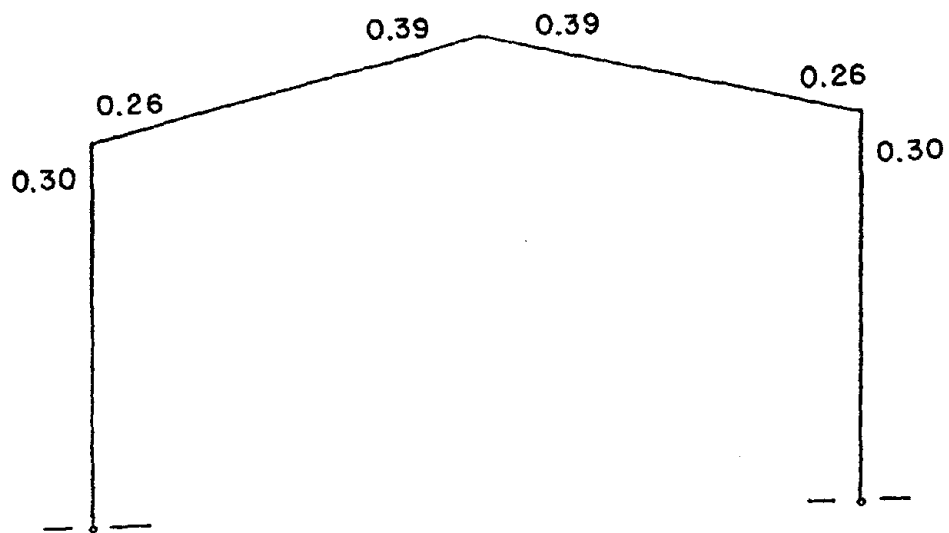
Corresponding to AISC Formula:

$$\frac{f_a}{f_a} + \frac{f_b}{f_b}$$

FIGURE 2-3 Design Ratio of Test Frame Under Gravity Load

SECTION 3

TEST FACILITY AND DATA ACQUISITION SYSTEM

The experiment was carried out using the shaking table at the State University of New York at Buffalo. The Table weighs 16.5 kips and has dimensions of 12 ft x 12 ft x 1 1/4 ft. The Table is a composite sandwich plate faced by ferrocement. It is vertically supported on four servo-hydraulic actuators and is connected to two horizontal actuators through swivel joints. The details of the shaking table facility are described in Refs. [7,17]. The system characteristics and the dynamic performance of the shaking table are presented in Ref. [9].

The data acquisition system used in this experimental investigation consists of a 64-channel MTS transducer conditioning system console (of which 12 channels were reserved for system control), a 30-channel Measurements Group 2100 conditioner and amplifier system, four 16-channel A/D (Analog–to–Digital) conversion subsystems, and a PDP-11 computer.

The four A/D conversion subsystems contain thirty-two 2-channel anti-aliasing filters, twenty 4-channel sample and hold cards, four 16-channel multiplexers, and four A/D converters. A typical A/D conversion subsystem is shown in Fig. 3–1. The maximum configuration of a typical A/D conversion subsystem is one 1230-1 (A/D-I) and four 1230-0 circuit (A/D-II) cards.

The A/D conversion subsystem has a data resolution of approximatly 5 mV based on the 12-bit digital word conversion. It is approximatly 0.05% of the maximum conditioner output of ± 10 Volts.

A special feature of the system is its ability to simultaneously sample the data by

FIGURE 3-1 A/D Conversion Subsystem
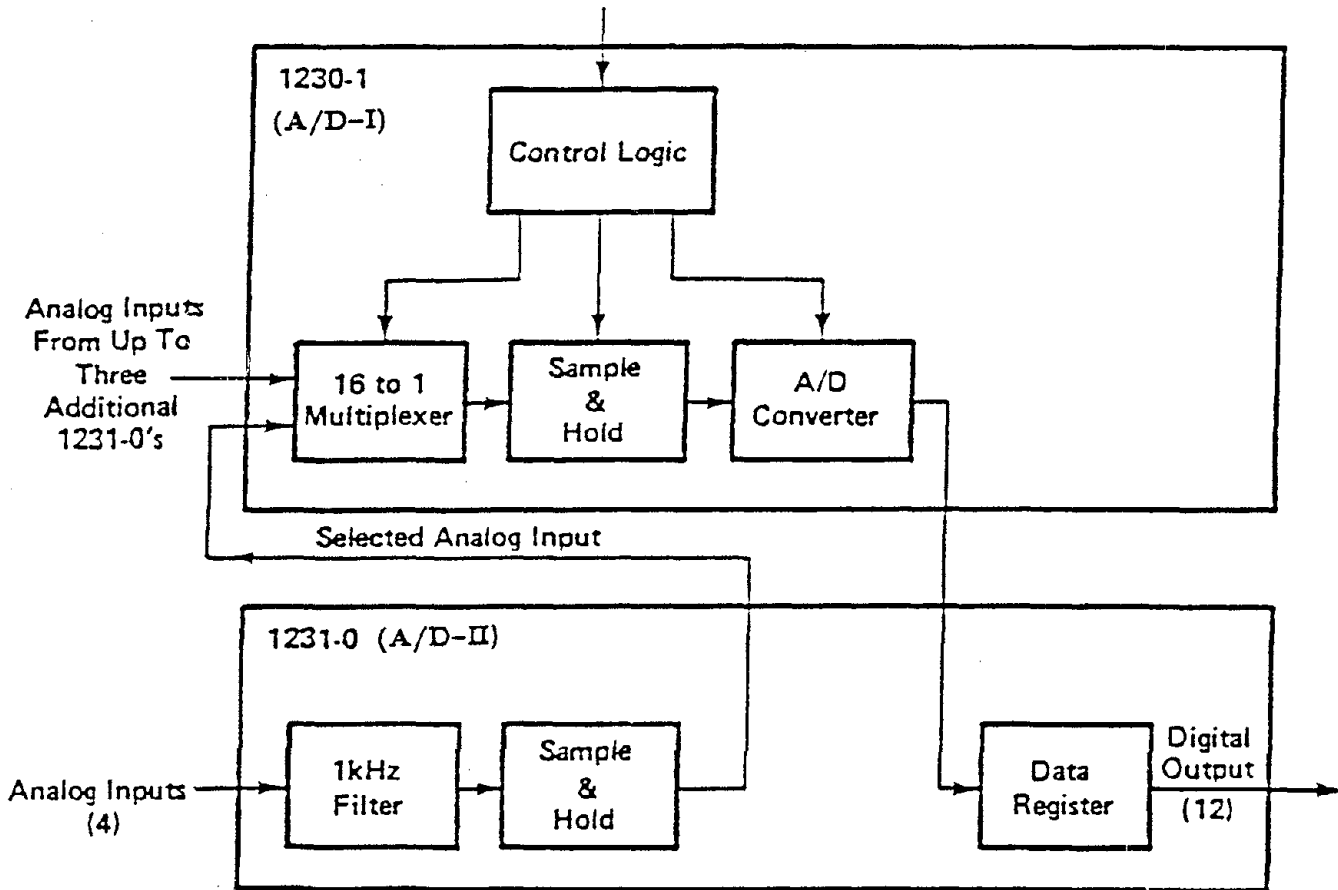
using four A/D conversion subsystems for a total of 64 data channels, with negligible phase lag. The maximum conversion time for each digital output is about 13 μsec so that the total required conversion time for the 64 channels is approximately 200 μsec. This is almost five times faster than the allowable minimum data time interval of 0.001 sec. limited by the seismic software.

SECTION 4

INSTRUMENTATION AND TEST PROGRAM

4.1 Instrumentation

Theoretically, instrumentation should only be necessary for one of the two "identical" parallel test frames. However, because of unavoidable variation between the two test frames, such as the material property and the fabrication process, full instrumentation was used on one frame and a limited amount of redundant instrumentation was used on the other. For better identification of the locations of the different transducers and other instrumentation, the various structural elements are identified according to their general location in the over-all test set-up. The total number of tranducer channels used were:

Strain gage bridges	26 channels
Accelerometers	13 channels
LVDT's	4 channels
Temposonics	4 channels

The summary of instrumentation is listed in Table 4–I. The typical locations of the various transducers in the west frame are also shown in Fig. 4–1.

4.2 Table Motions

Two earthquake ground motions, the S00E component of the 1940 El Centro Earthquake (ELC) and the S69E component of the 1952 Taft Earthquake (TF), were used in this study. The Taft earthquake was used only for the preliminary test for validating instrumentation and for identifying the fundamental dynamic properties

Table 4-I Instrumentation Scheme

Channel No.	Channel File Identification	Signal
52	MTS 450	Flexural and axial strains, SW column
51	MTS 450	Flexural and axial strains, NW column
50	MTS 450	Flexural and axial strains, SW rafter
49	MTS 450	Flexural and axial strains, NW rafter
48	MTS 450	Flexural and axial strains, SW column
47	MTS 450	Flexural and axial strains, NW column
46	MTS 450	Flexural and axial strains, SW rafter
45	MTS 450	Flexural and axial strains, NW rafter
44	MTS 450	Flexural strain, SW column
43	MTS 450	Flexural strain, SW column
42	MTS 450	Flexural strain, SW rafter
41	MTS 450	Flexural strain, SW rafter
40	MTS 450	Flexural strain, NW column
39	MTS 450	Flexural strain, NW column
38	MTS 450	Flexural strain, NW rafter
37	MTS 450	Flexural strain, NW rafter
36	B&K 4370, 949970; ch. E3	Out-of-plane acceleration, SE column
35	B&K 4370, 947929; ch. D9	Out-of-plane acceleration, NE column
34	B&K 4370, 949927; ch. D8	Out-of-plane acceleration, roof ridge
33	MTS 450	Flexural and axial strains, NE column
32	MTS 450	Flexural and axial strains, SE column
31	MTS 450	Flexural strain, SE column
30	MTS 450	Flexural strain, SE column
29	MTS 450	Flexural strain, SE column
28	MTS 450	Flexural strain, SE column
27	MTS 450	Flexural strain, SE rafter
26	MTS 450	Flexural and axial strains, NE column
25	MTS 450	Flexural strain, NE rafter
24	MTS 450	Flexural and axial strain, NE column

Table 4-I Instrumentation Scheme (Cont'd)

Channel No.	Channel File Identification	Signal
23	Endevco S/N NP74, ch. A6	In-plane acceleration, SE column top
22	LVDT, S/N 2209	SE panel zone deformation
21	LVDT, S/N 2202	SE panel zone deformation
20	LVDT, S/N 1692	NE panel zone deformation
19	LVDT, S/N 1691	NE panel zone deformation
18	Temposonic	Base rotation, NE column bottom
17	Temposonic	Absolute Displacement, NW column top
16	Endevco S/N PP34, ch. A0	Vertical accel., SE found. corner
15	Endevco S/N LN91, ch. A1	Horizontal accel., SE found. corner
14	Endevco S/N PP96, ch. A9	Horizontal accel., NW found. corner
13	Endevco S/N FW42, ch. A3	Vertical accel., NW found. corner
12	Endevco S/N NP64, ch. C3	In-plane acceleration, NW column top
11	Endevco S/N RB95, ch. D4	In-plane acceleration, NE column top
10	Endevco S/N PS73, ch. A5	Vertical acceleration, Middle of ridge
09	Temposonic	Absolute displacement, NE column top
08	Temposonic	Base rotation, SW column bottom
07	Endevco S/N PK59, ch. A7	Horizontal accel., Middle of ridge
06	Endevco S/N PE61, ch. A8	In-plane acceleration, SW column top
05	MTS 450	Axial strain, NW column web
04	MTS 450	Axial strain, SW column web
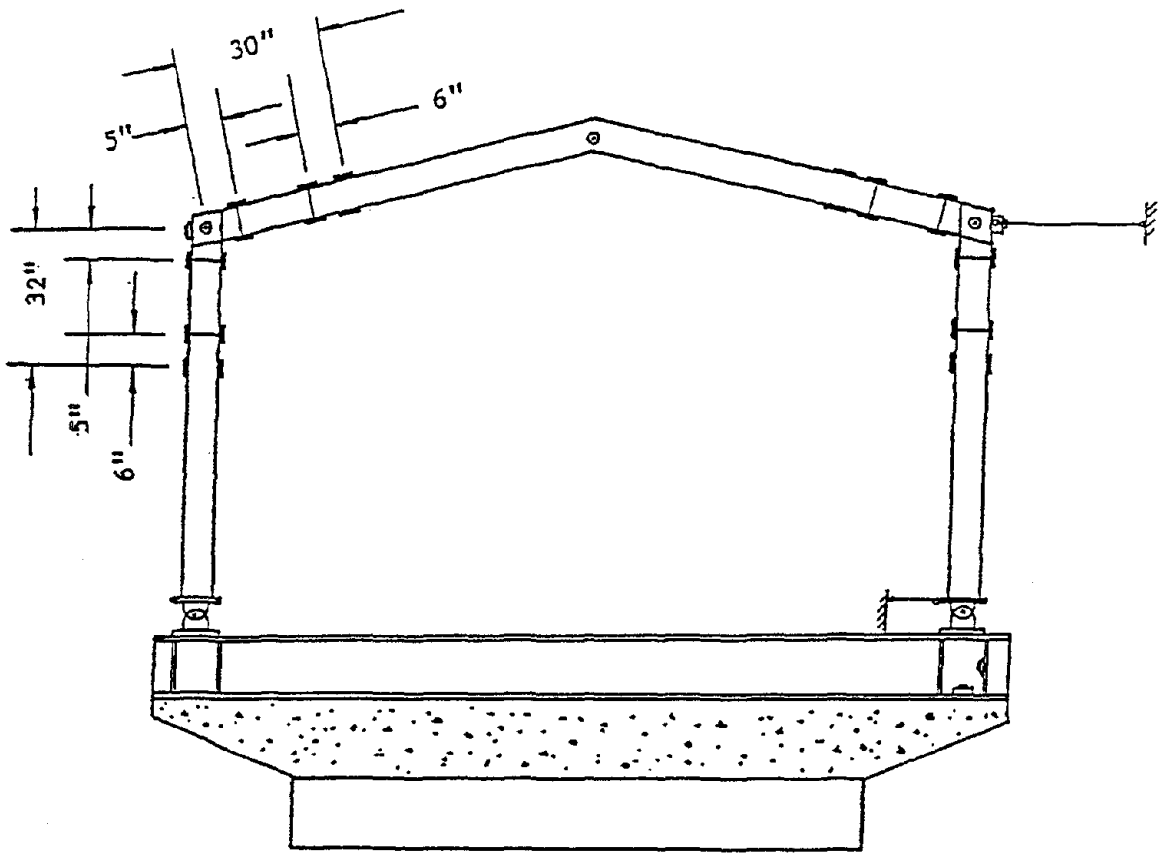
| | : strain gage - quarter bridge   (for axial strain and flexural strain) |

H : strain gage - half bridge   (for flexural strain)

θ : in-plane accelerometer (Endevco)

⊙ : out-of-plane accelerometer (B&K)

⊶ : Temposonic (MTS)

FIGURE 4-1 Typical Transducers on West Frame

of the test structure. The El Centro Earthquake was used to study the linear and nolinear behavior of the test structure. These two ground motions were corrected using a modified frequency domain data processing before they were introduced to the control console of the shaking table [9].

After the first series of tests was completed, the structure was retrofitted and the time step of the ELC earthquake was scaled by the ratio of the first mode natural frequencies of the test structures before and after retrofit. Thus, with respect to the input response spectrum, the test structures before and after retrofit were subjected to equal spectrum values corresponding to their first mode natural frequencies.

4.3 Test Sequence

The test sequence consists of two phases. The first phase was performed with the original test structure. After the structure had been subjected to severe inelastic deformation, the test was stopped and the test structure was retrofitted. The second series was carried out to study the feasibility and efficiency of one particular type of retrofit, with a simple type of knee brace. The test sequences of both phases are given in Table 4–II.

For the original test structure, a total of eleven earthquake excitation tests were performed, covering the entire range of elastic and inelastic behavior. Two of the eleven excitations were carried out to identify the basic dynamic properties of the test structure, such as the natural frequency and the damping ratio. In addition, a few small-amplitude, banded white noise tests were carried out to investigate the natural frequency change of the test structure during the tests.

At the beginning of the first phase tests, two scaled earthquake ground motions, ELC with 0.15 g peak acceleration and TF with 0.10 g peak acceleration, were

Table 4-II Test Sequences

Before Retrofit	After Retrofit
0.15 g peak ELC 0.10 g peak TF banded white noise	banded white noise
0.10 g peak ELC 0.20 g peak ELC 0.30 g peak ELC 0.35 g peak ELC 0.50 g peak ELC 0.60 g peak ELC 0.70 g peak ELC banded white noise 0.80 g peak ELC (i) banded white noise 0.80 g peak ELC (ii) banded white noise	0.10 g peak ELC 0.20 g peak ELC 0.35 g peak ELC 0.50 g peak ELC 0.60 g peak ELC 0.70 g peak ELC 0.80 g peak ELC banded white noise 0.90 g peak ELC (i) banded white noise 0.90 g peak ELC (ii) banded white noise

employed to define the fundamental dynamic properties of the test structure by using the "system identification" method [18,19]. In addition, two small-amplitude, banded white noise tests with frequency contents of [0 Hz – 25 Hz] and [0 Hz – 5 Hz] were used to identify the dynamic properties using the HP Spectrum Analyser. (The white noise with a frequency content of [0 Hz – 5 Hz] was used to increase the resolution of the measured first mode natural frequency of the test structure. The resolution was then made equal to 0.0244 Hz corresponding to the 12-bit digital conversion.)

Nine test runs with various peak accelerations of 0.10 g to 0.80 g of ELC earthquake were next performed. This was done to determine the behavior of the test structure subjected to elastic, moderately inelastic and severely inelastic deformations, and to obtain the ultimate lateral strength of the test structure. This latter condition was experimentally defined, and corresponded to that condition where the maximum story drift in two consecutive test runs increased continuously while the maximum base shear force decreased or remained constant. At that stage, the test sequence was stopped.

The structure was then repaired, and the basic dynamic properties of the "retrofitted structure" were identified using the Spectrum Analyser and banded white noise excitation. Once the first mode natural frequency of the repaired structure was identified, the time step of the input ELC earthquake was scaled as described above. Thereafter, a total of nine test runs (0.10 g — 0.90 g time-scaled ELC) were performed with a process similar to the one used in the first phase.

SECTION 5

TEST RESULTS

Results of three of the test runs, 0.15 g peak ELC, 0.60 g peak ELC and 0.80 g peak ELC (ii) are discussed in this report. These three test runs correspond to, respectively, elastic, moderately inelastic and severely inelastic behavior of the test frame. For the retrofitted structure, the envelope curve of all tests was compared with that of the original structure.

For numerical predictions, the general purpose computer program, DRAIN-2D [13] and an average yielding stress of 42 ksi obtained from material coupon tests were used.

5.1 Dynamic Characteristics of the Test Structure

An input of a small-amplitude, banded white noise with frequency content of 0 – 25 Hz was first introduced to excite the test structure in the N-S (in-plane) direction. The horizontal accelerations at the column tops and the roof ridge in the in-plane direction were measured. The transfer function and phase angles were obtained by using a HP 3582A Spectrum Analyzer. The fundamental natural frequency in the N-S direction was observed to be 2.2 Hz, as can be seen in Fig. 5-1(a). The other two (much smaller) peak values occurred approximately at 7.8 Hz and 22.5 Hz, and were considered to be the frequency of the torsional mode of the the test structure and the frequency of the rolling mode of steel-concrete foundation. At 7.8 Hz, the phase angle between the two measured accelerations at NW and NE column tops was of 178 degree. (It is therefore considered to be the torsional mode of the test structure.) The transfer function of the vertical acceleration at the NW corner of

the foundation to the table horizontal acceleration is shown in Fig. 5–1(b). From the figure, it may be estimated that the foundation has its first–mode frequency around 22.5 Hz with respect to the test structure placed on it.

To have better resolution in using the spectrum analyzer, a 0 – 5 Hz white noise was introduced and the test was repeated. For that case, the natural frequency was estimated to be 2.08 Hz, and the damping ratio determined by the half-power method was 1.92 %.

Results of the "system identification" method [18,19] indicated that the natural frequency and the damping ratio of the test structure were 1.97 Hz and 1.66 % for the 0.15 g peak ELC test, and 1.99 Hz and 2.88 % for the 0.10 g peak TF test. Identified structural responses are compared with measured structural responses in Figs. 5–2 and 5–3.

5.2 Shaking Table Performance

Because the reaction force and the resonance of the test structure may affect the accuracy of the feed–back control of the shaking table, this effect was investigated during the experiment. In Fig. 5–4, the desired and achieved acceleration time histories and corresponding response spectra with respect to 0.15 g peak ELC, 0.60 g peak ELC and 0.80 g peak ELC (ii) tests are presented. As can be seen from these figures, the pattern of the effect of table-structure interaction is the distortion at a few peaks of the acceleration time history. The distortion became more obvious with increasing intensity of excitation as the reaction force of the test structure on the shaking table became larger. Also to be noted, the loss of accuracy was primarily confined to the high frequency range. Furthermore, the distortion in the acceleration time history at a few peaks showed the instants when the structure

experienced moderate to severe damage.

5.3 Behavior of Test Structure

For the elastic test with 0.15 g peak ELC, the structural symmetry was preserved both for the global (displacements measured at the column tops) and local (curvatures measured at the column tops and rafter ends around the column-to-rafter joints) responses. The typical local hysteresis curves shown in Fig. 5-5 demonstrates the linearity of elastic response.

In the moderate inelastic test with 0.60 g peak ELC, permanent offsets were observed in the local responses. From a global response view point, these permanent offsets were not obvious. The local hysteresis curves at four critical sections — rafter ends and column tops — are shown in Fig. 5-6. From this figure, the non-uniform distribution of inelastic deformation over the four critical sections is obvious, and the local structural symmetry is no longer preserved.

In the final test run, 0.80 g peak ELC (ii), local buckling occurred at the column top, and a kinematic structural mechanism nearly formed with a 1.5 inch permanent sidesway at the column top, as shown in Fig. 5-7. The local hysteresis curves shown in Fig. 5-8 reveal that the inelastic deformation is more uniformly distributed over four critical sections than that of the 0.60 g peak ELC test.

The envelope of maximum base shear force versus the maximum story drift corresponding to each test in the test program is shown in Fig. 5-9. Based on this figure, the maximum lateral strength of the test frame can be obtained. It is interesting to observe that the envelope curve shows a "transition zone" around the 0.5 g peak ELC and 0.6 g peak ELC tests. Beyond this "transition zone", the slope of the envelope curve decreases rapidly. Before the "transition zone", the structure

resisted the seismic force primarily by its lateral over-strength. The simultaneous formation of a sufficient number of plastic hinges for the formation of a collapse mechanism limited the further strength development after this "transition zone".

5.4 Numerical Prediction

For the 0.15 g peak ELC test, the analytical prediction suggests that the consideration of semi-rigid joints is required even when the panel zones are properly stiffened with two doubler-plates. The mathematical models and the numerical results are shown in Fig. 5–10. The masses lumped at each column top and the roof ridge are assumed to be 1/4 m and 1/2 m , respectively, where m is the total seismically reactive mass on the test frame.

For the moderate inelastic test, 0.60 g peak ELC test, the theoretical prediction is given in Fig. 5–11. For the severe inelastic deformation test (0.80 g peak ELC (ii) test), the numerical prediction is given in Fig. 5–12(a). The comparison of the numerical results with and without the consideration of semi-rigid joint, shown in Fig. 5–12(b), suggests that the semi-rigid joint may be less important in the prediction of inelastic response. This is because the pinned-base steel gable frame possessed only one degree of structural redundancy, and the formation of a sufficient number of plastic hinges (a minimum of 2) was simultaneous with the formation of a structural mechanism. The inelastic deformation at the critical sections contributed dominantly to the global structural response.

5.5 Test Results of Retrofitted Structure

After the first set of tests, the structure was repaired to study the feasibility and appropriateness of a particular type of retrofit. Two knee braces were added

to bypass the zones where severe inelastic deformation had previously occurred. A profile of this retrofit was finally decided and is shown in Fig. 5-13.
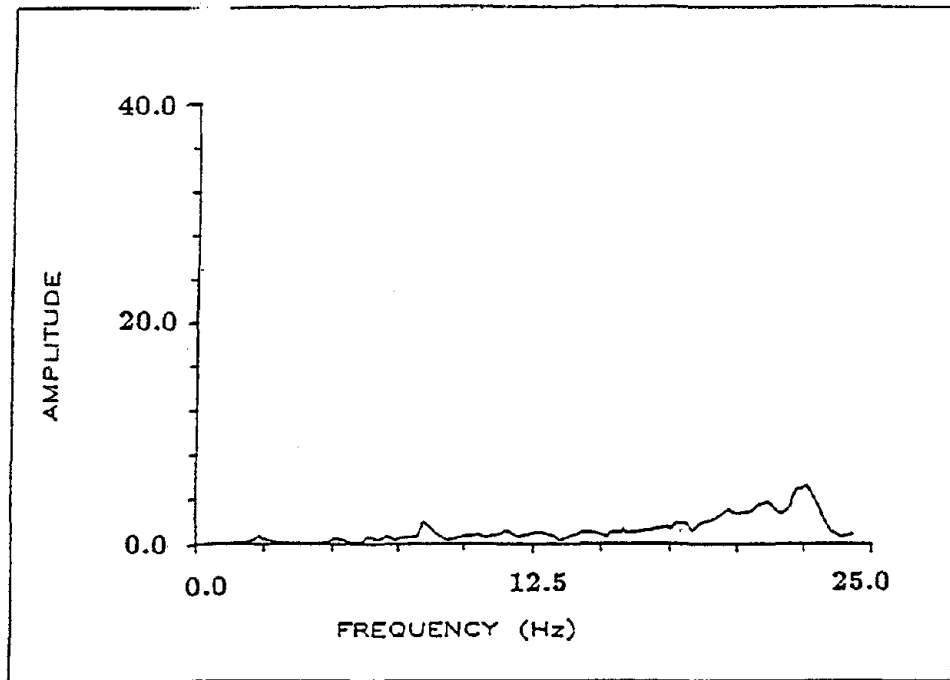
The fundamental frequency of the repaired structure was determined to be 2.52 Hz, using the Spectrum Analyzer test. The damping ratio was about 1.4%.

For the final test (0.90 g peak ELC (ii) test), the local hysteresis curves are shown in Fig. 5-14. From these figures, it is interesting to observe that the severe inelastic deformations are concentrated in only three critical sections. Particularly, two of them are more exaggerated. The maximum base shear force obtained in this test was slightly less than the previous 0.90 g peak ELC (i) test, as shown in Fig. 5-15. When the repaired structure reached its ultimate lateral strength (at 0.90 g peak ELC (ii) test), local flange buckling was observed. Web buckling was not present.

TRANSFER FUNCTION

AT COLUMN SE TOP

Column Top

FIGURE 5-1(a) Transfer Function of Measured Acceleration to Banded White Noise Input

at NW Corner

FIGURE 5-1(b) Transfer Function of Measured Vertical Acceleration at Steel Foundation to
Horizontal Banded White Noise Input (0.25 Hz)

(a) at NW Column Top - 0.15 g Peak ELC
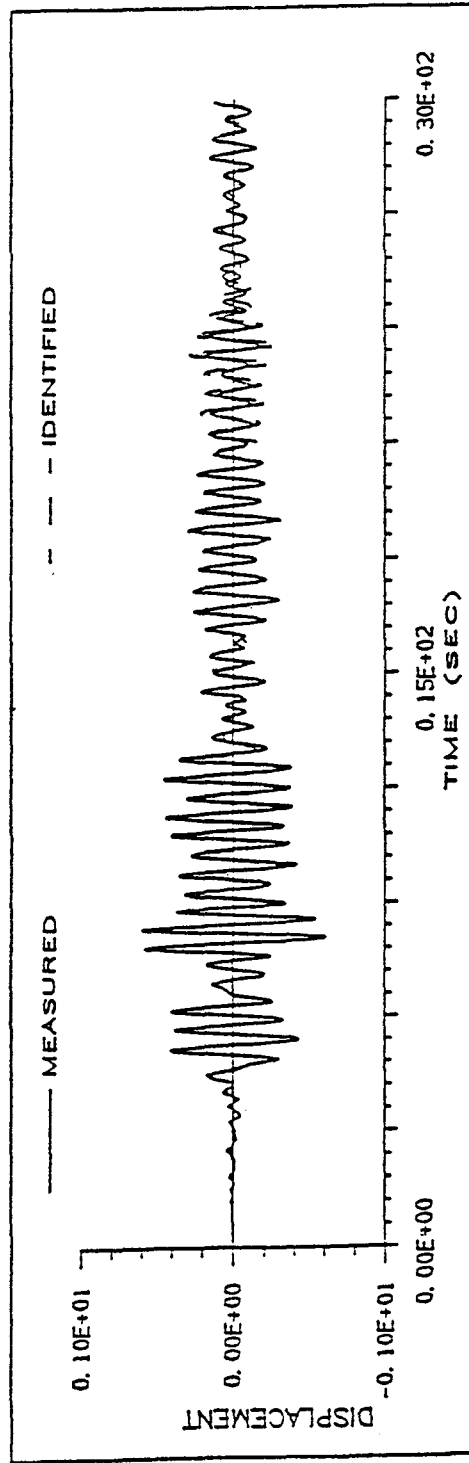
(b) at NW Column Top - 0.10 g Peak TF

FIGURE 5-2 Comparison of Measured Relative Displacement and Identified Relative
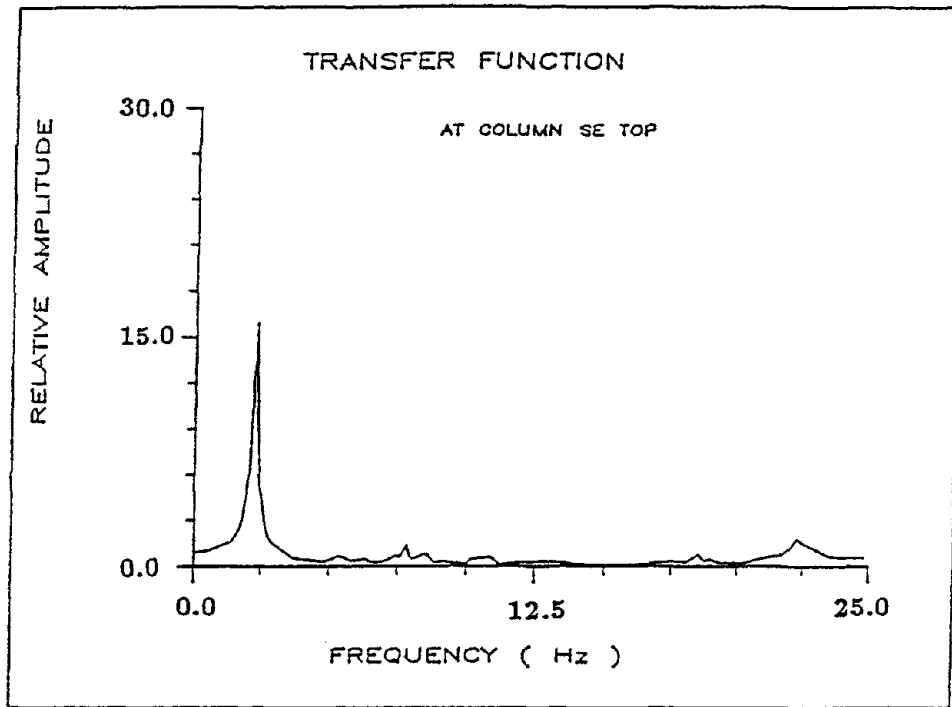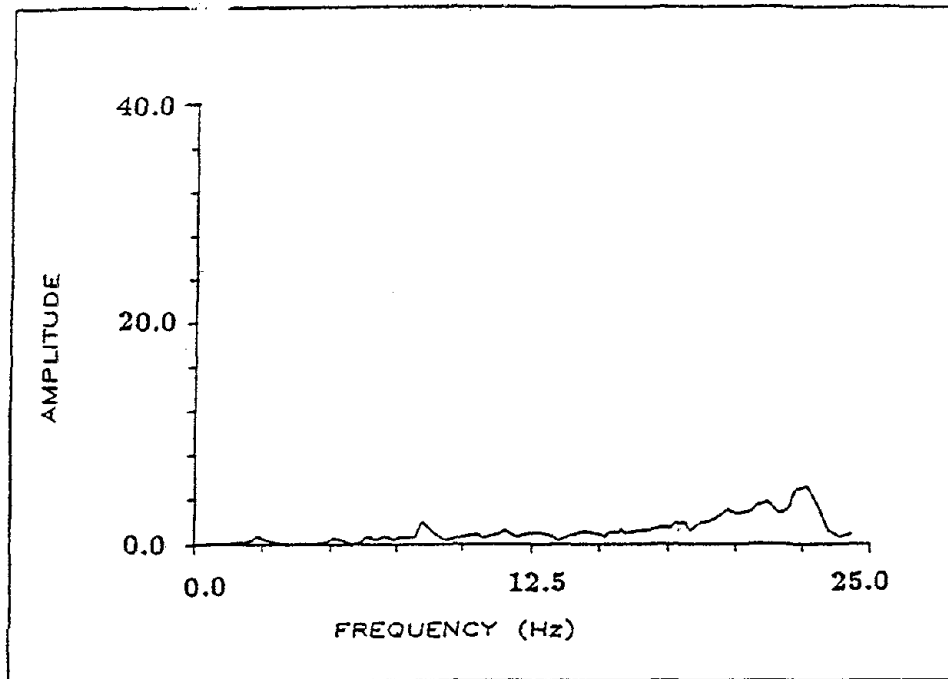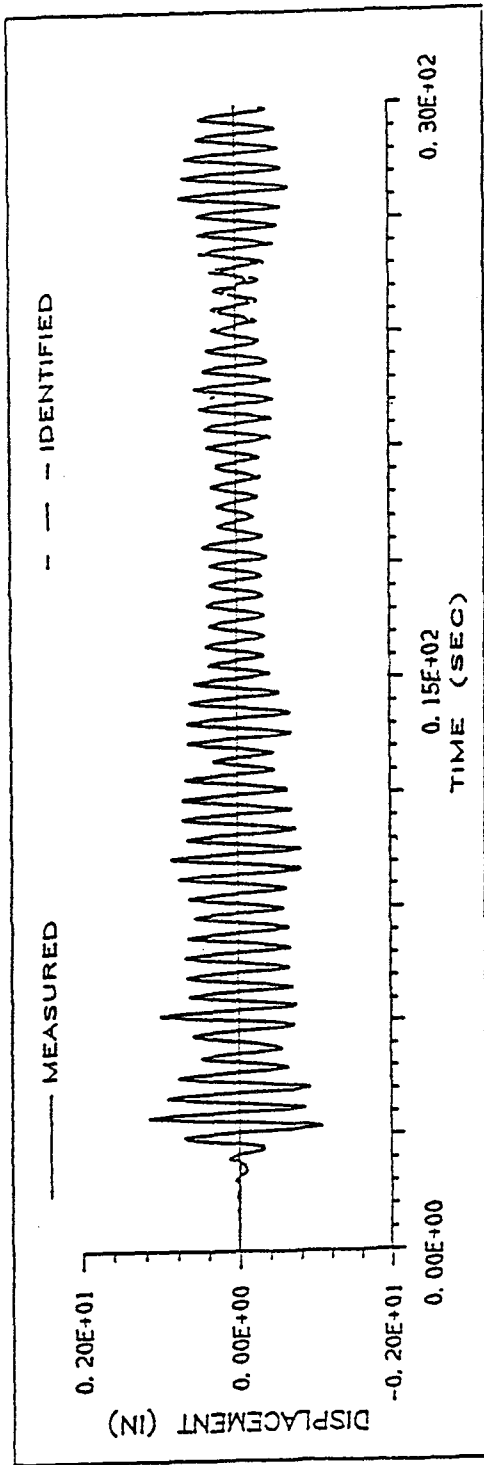Displacement
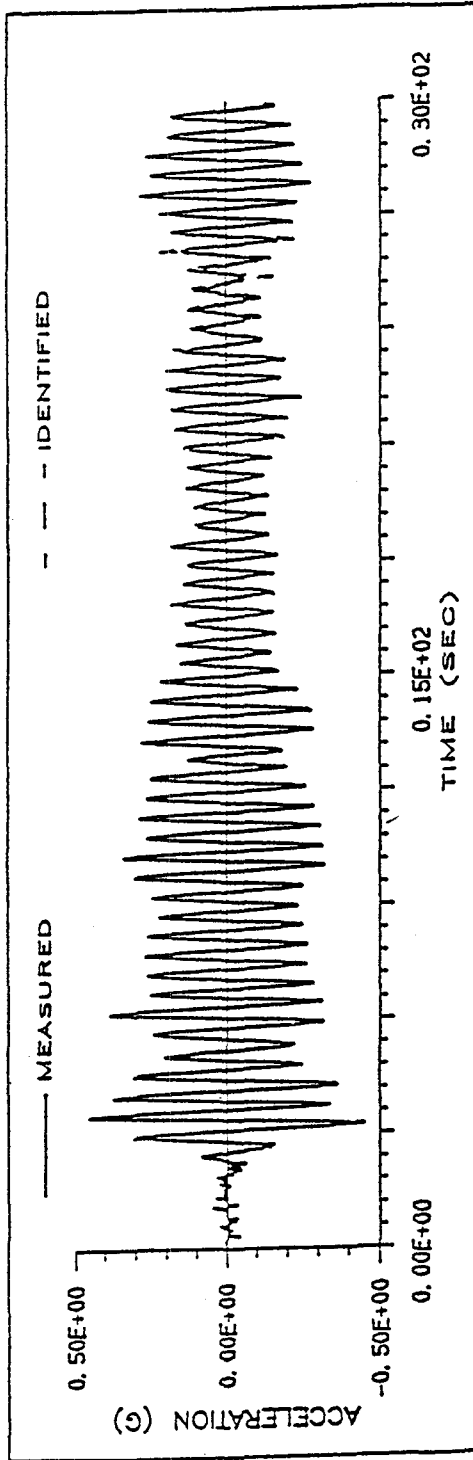
(a) at NW Column Top - 0.15 g Peak ELC
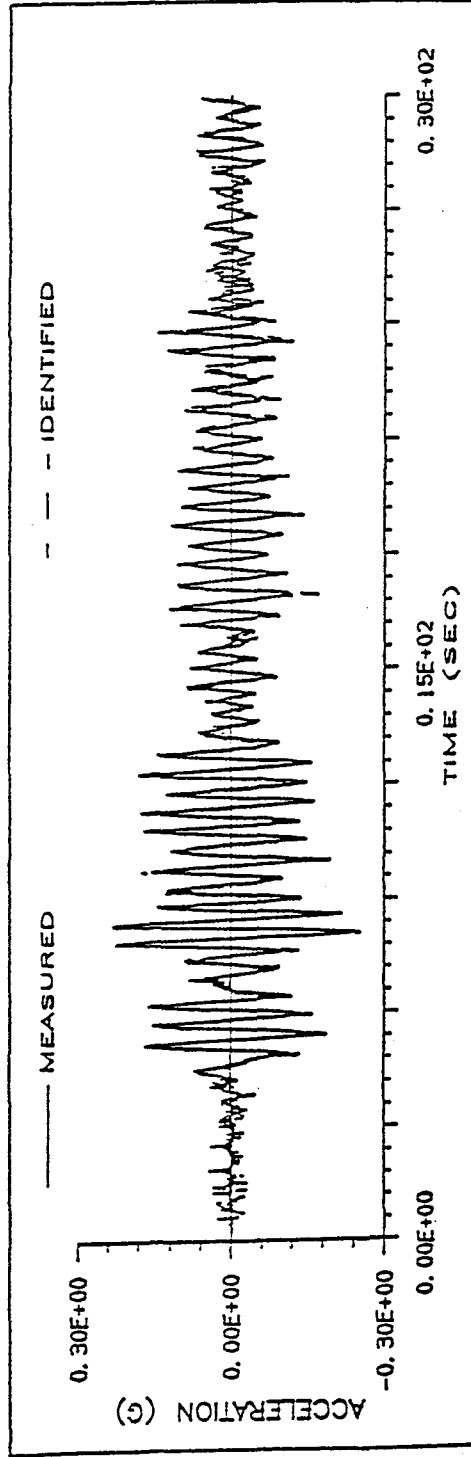
(b) at NW Column Top - 0.10 g Peak TF

FIGURE 5-3 Comparison of Measured Acceleration and Identified Acceleration

to bypass the zones where severe inelastic deformation had previously occurred. A profile of this retrofit was finally decided and is shown in Fig. 5-13.

The fundamental frequency of the repaired structure was determined to be 2.52 Hz, using the Spectrum Analyzer test. The damping ratio was about 1.4%.

For the final test (0.90 g peak ELC (ii) test), the local hysteresis curves are shown in Fig. 5-14. From these figures, it is interesting to observe that the severe inelastic deformations are concentrated in only three critical sections. Particularly, two of them are more exaggerated. The maximum base shear force obtained in this test was slightly less than the previous 0.90 g peak ELC (i) test, as shown in Fig. 5-15. When the repaired structure reached its ultimate lateral strength (at 0.90 g peak ELC (ii) test), local flange buckling was observed. Web buckling was not present.

TRANSFER FUNCTION

AT COLUMN SE TOP

Column Top

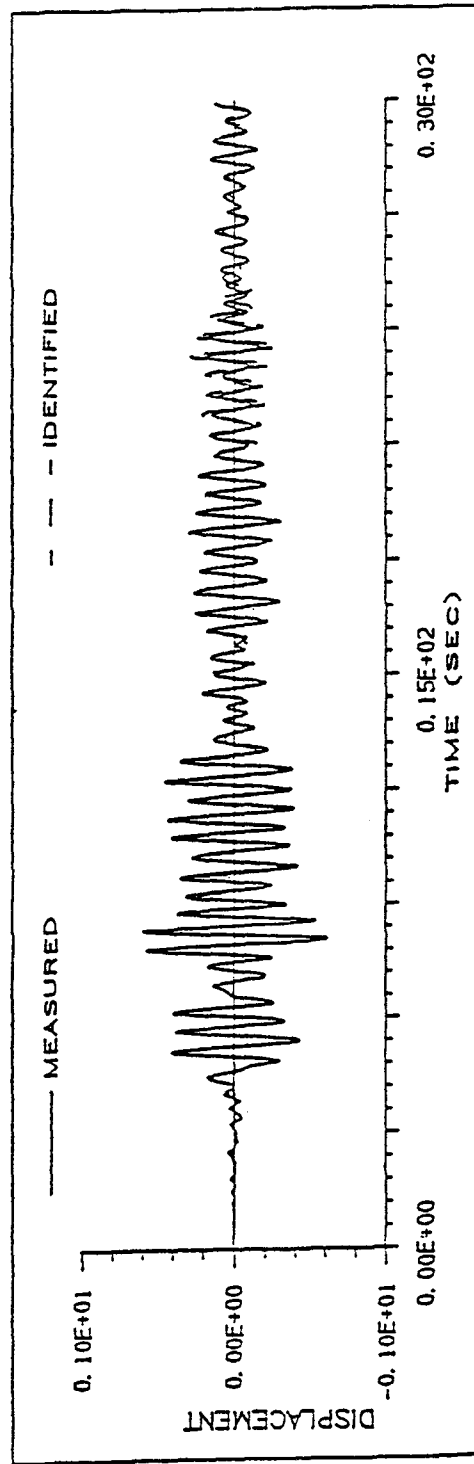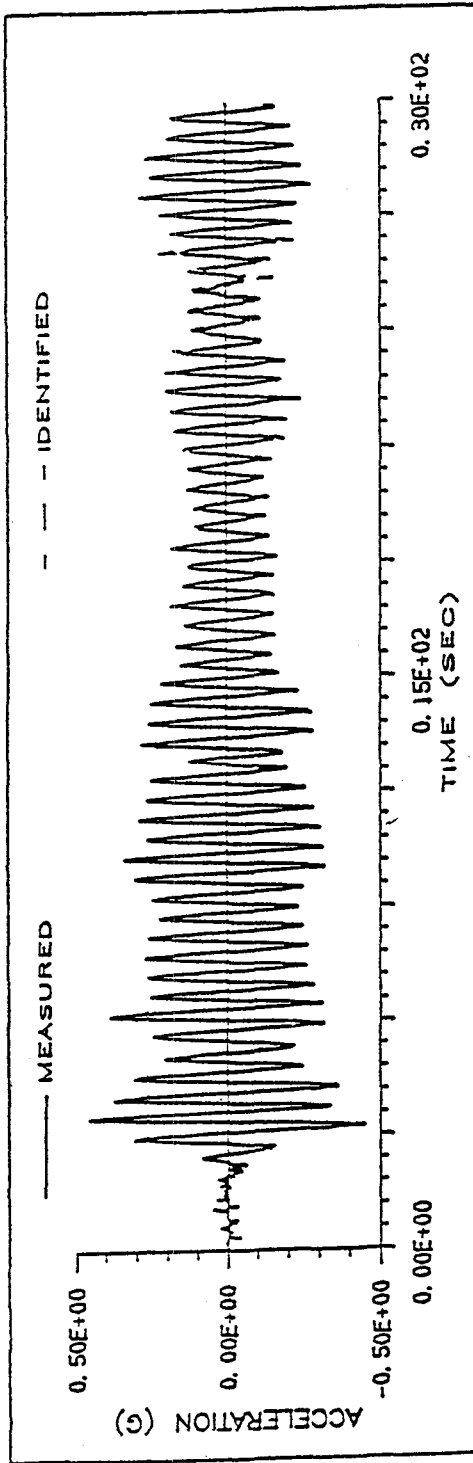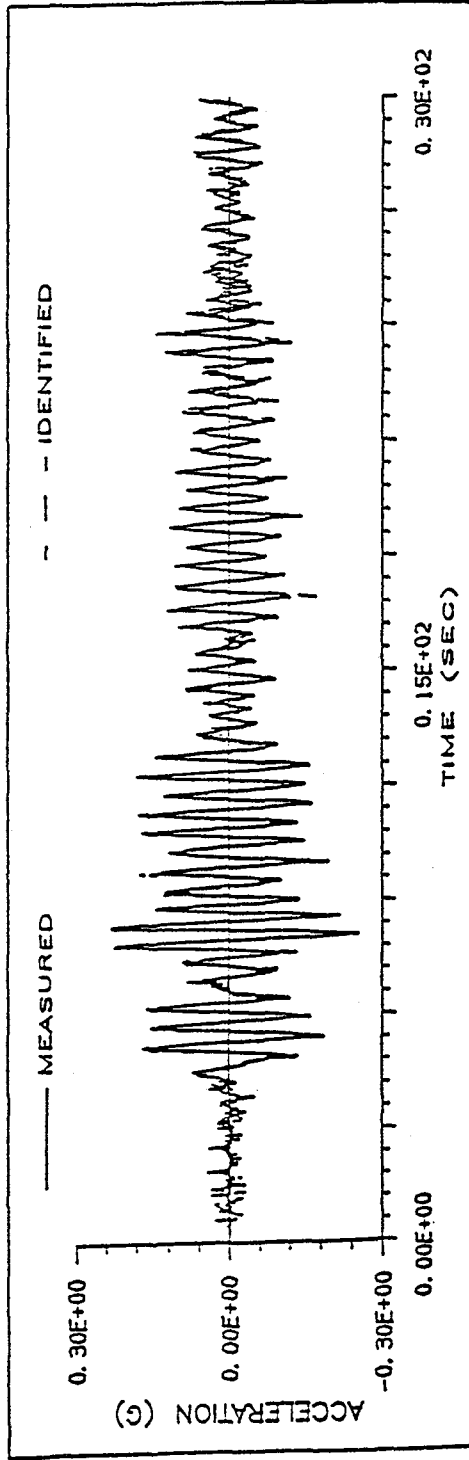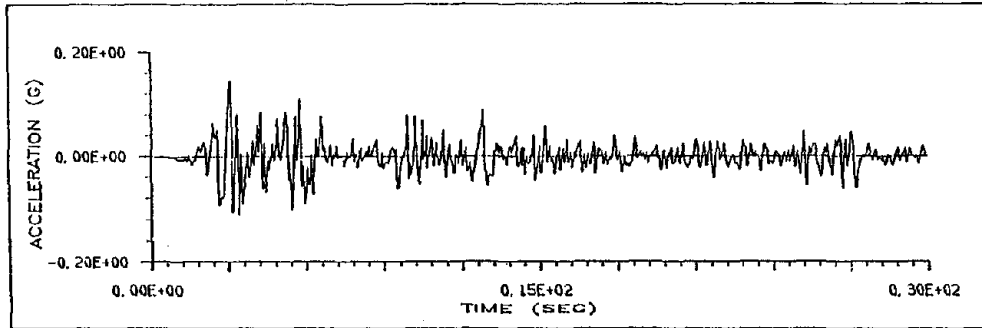FIGURE 5-1(a) Transfer Function of Measured Acceleration to Banded White Noise Input

at NW Corner

FIGURE 5-1(b) Transfer Function of Measured Vertical Acceleration at Steel Foundation to Horizontal Banded White Noise Input (0.25 Hz)

5-6

(a) at NW Column Top - 0.15 g Peak ELC

(b) at NW Column Top - 0.10 g Peak TF

FIGURE 5-2 Comparison of Measured Relative Displacement and Identified Relative
Displacement

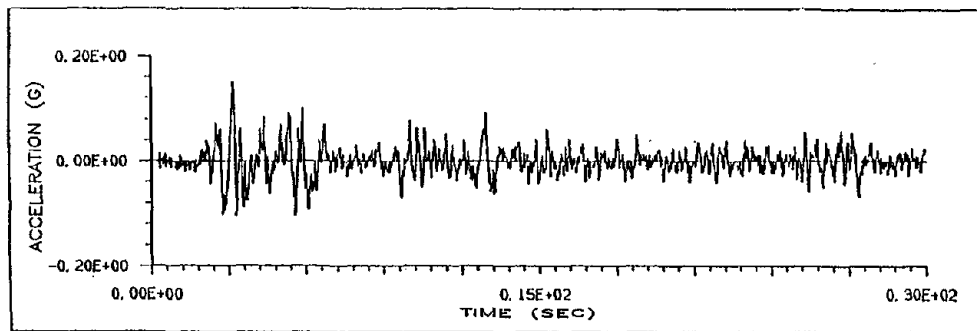(a) at NW Column Top - 0.15 g Peak ELC
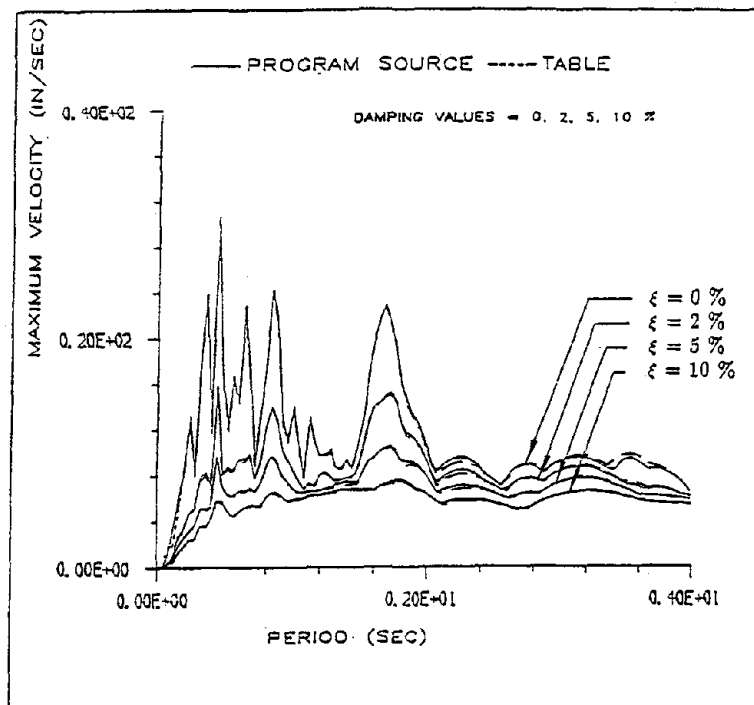

(b) at NW Column Top - 0.10 g Peak TF

FIGURE 5-3 Comparison of Measured Acceleration and Identified Acceleration
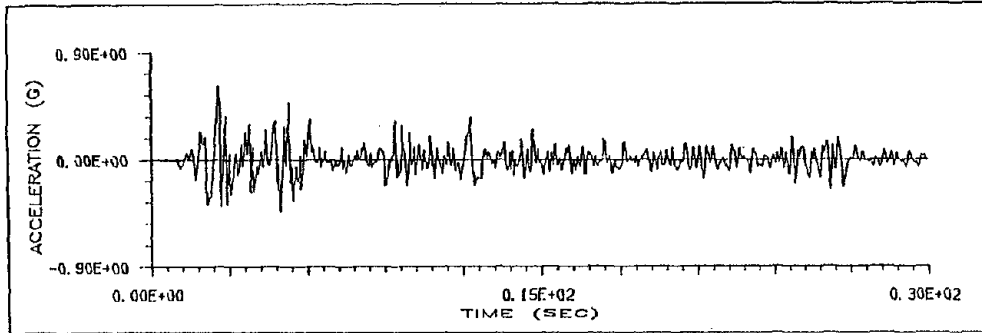
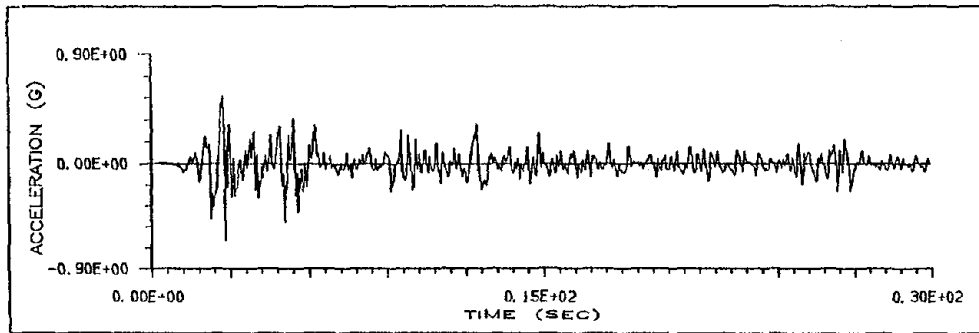(a.1) Input Table Acceleration

(a.2) Measured Table Acceleration
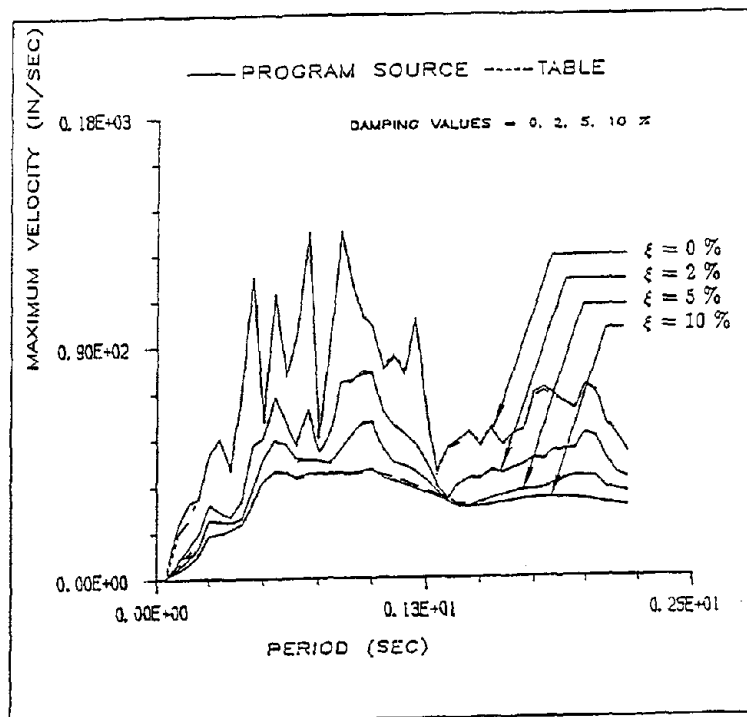

(a.3) Response Spectra

FIGURE 5-4(a) Comparison of Input and Measured Table Motions - 0.15g Peak ELC Test
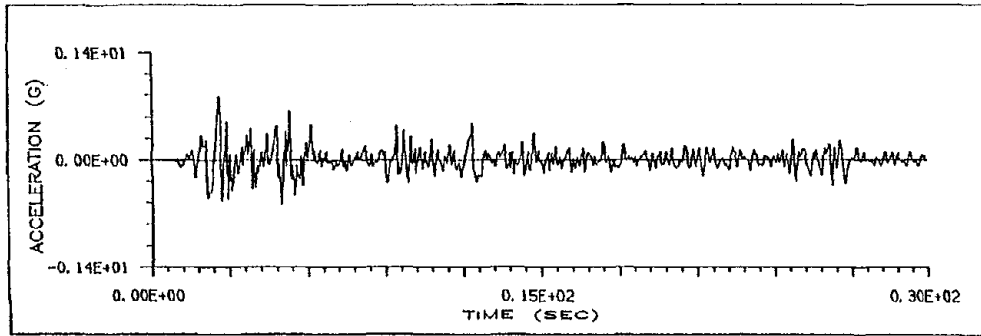
(b.1) Input Table Acceleration

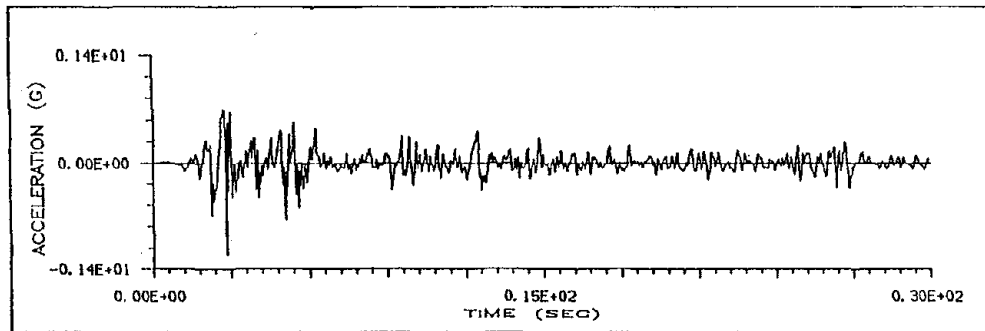**(b.2) Measured Table Acceleration**

(b.3) Response Spectra

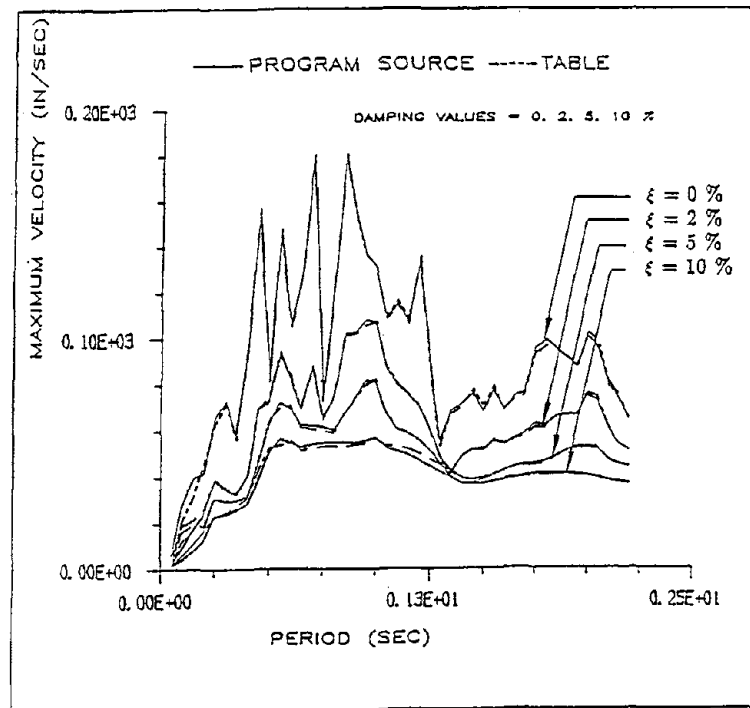FIGURE 5-4(b) Comparison of Input and Measured Table Motions - 0.60g Peak ELC Test

5-10

(c.l) Input Table Acceleration

(c.2) Measured Table Acceleration
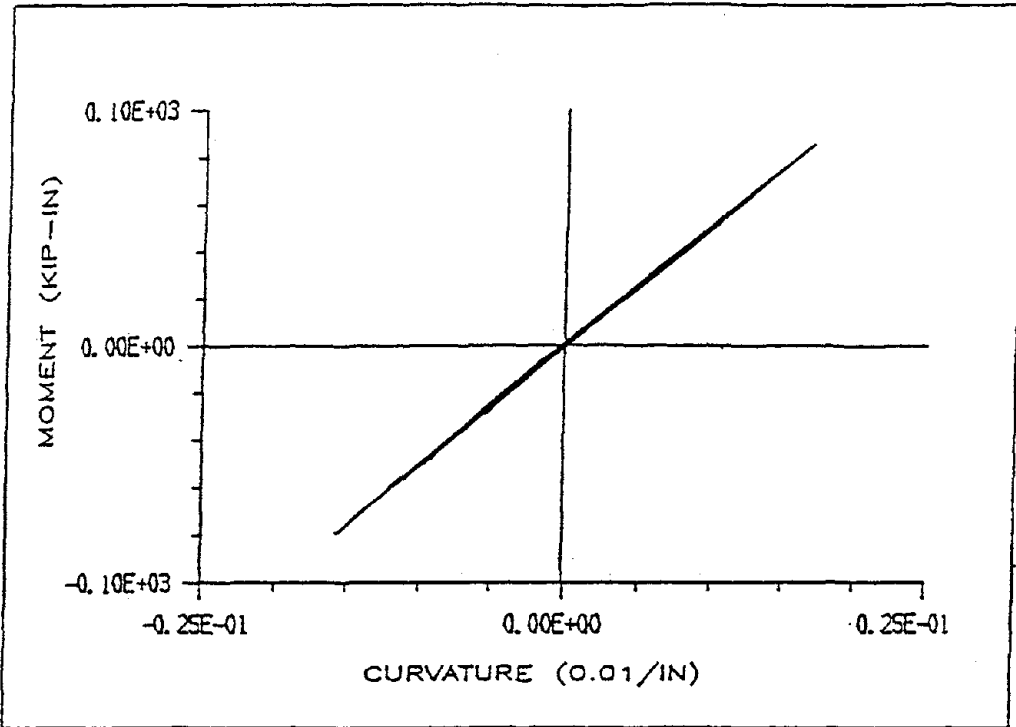

(c.3) Response Spectra

FIGURE 5-4(c) Comparison of Input and Measured Table Motions - 0.80g Peak ELC (ii) Test

5-11
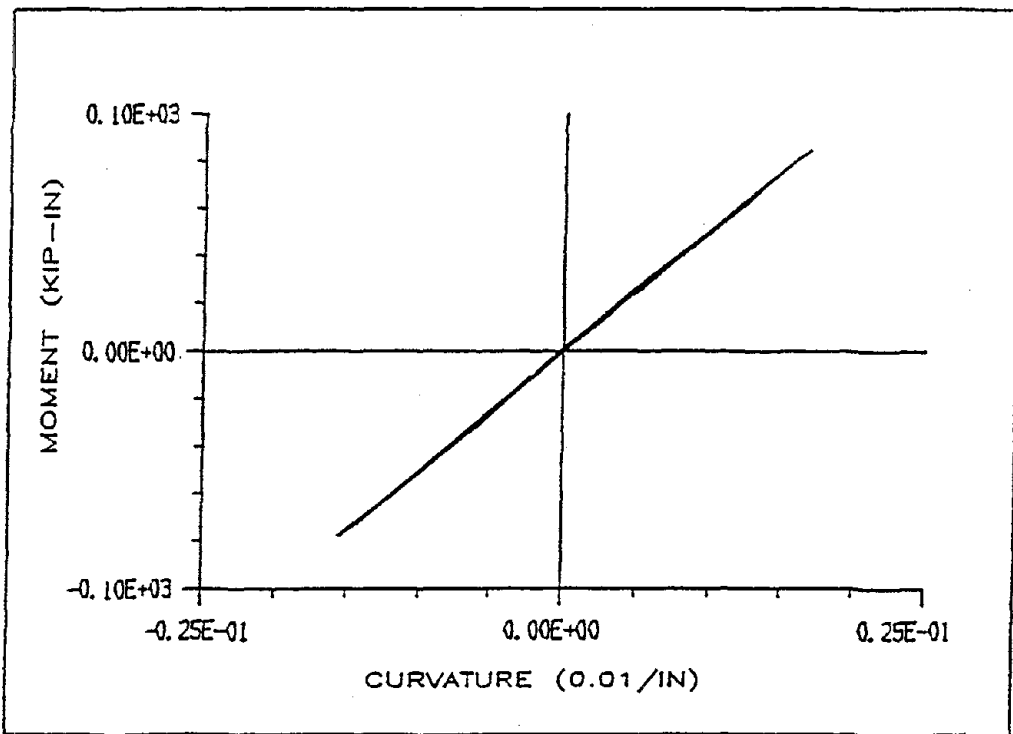
(a) at SW Column Top

(b) at NW Column Top

FIGURE 5-5 Hysteresis Curve of Section Moment vs. Curvature - 0.15g Peak ELC
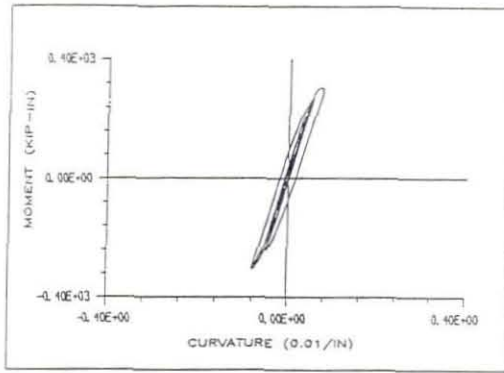
(a) NW Column Top
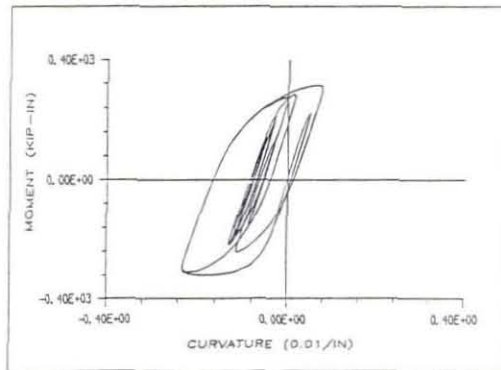
(b) SW Column Top
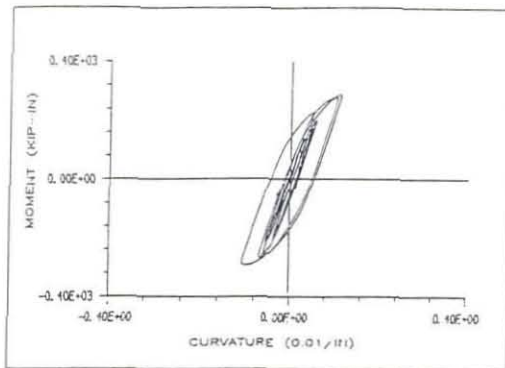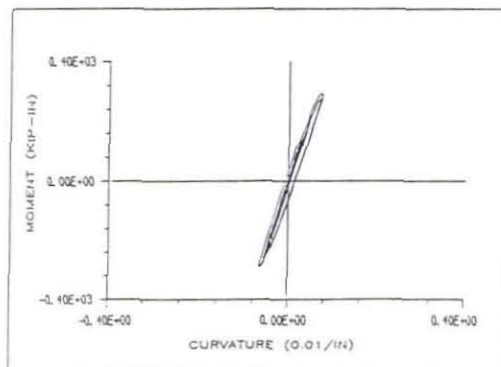
(c) NW Rafter End

(d) SW Rafter End

FIGURE 5-6 Local Hysteresis Curves - 0.60g Peak ELC Test

5-13
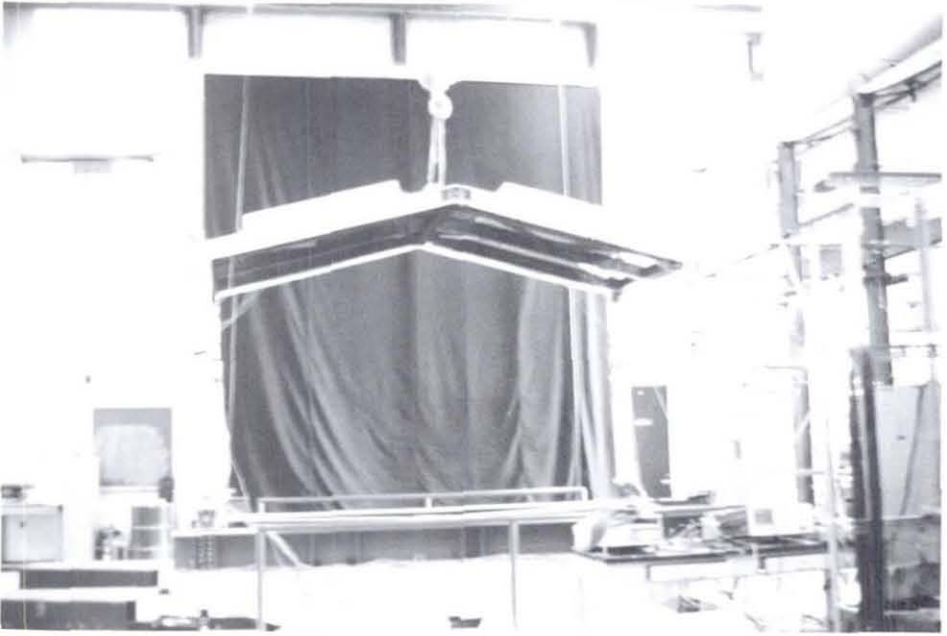
(a) Global Permanent Sidesway
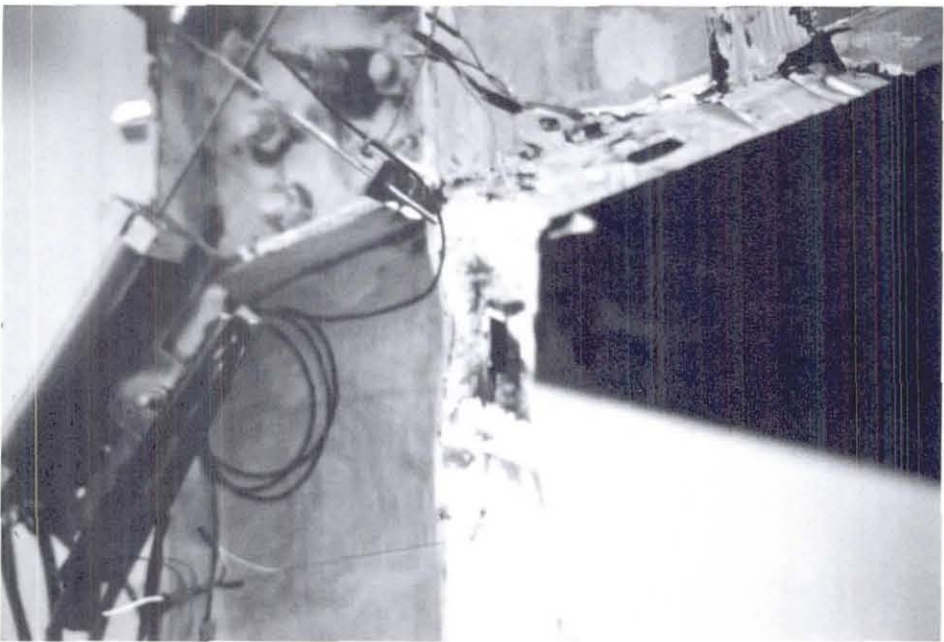
(b) Local Buckling at SW Column Top

FIGURE 5-7 Local and Global Damage - 0.80g Peak ELC (ii) Test
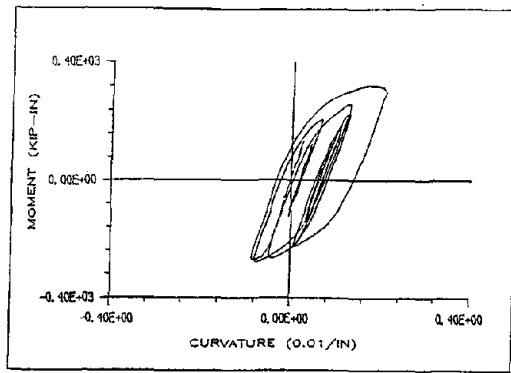
(a) NW Column Top
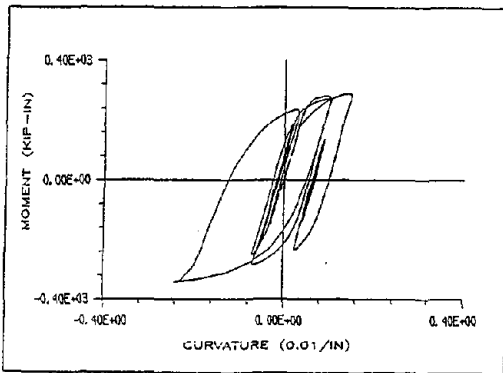
(b) SW Column Top
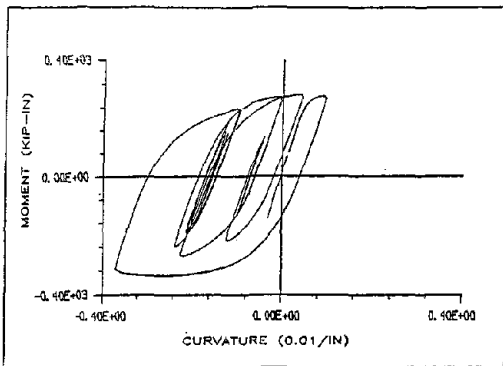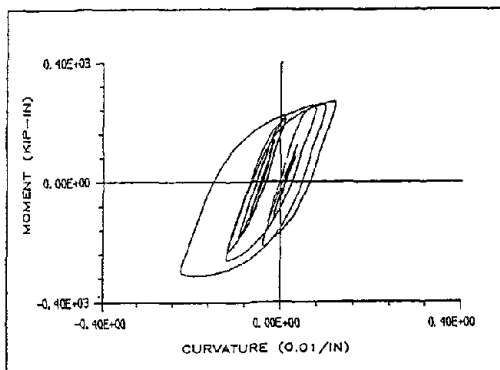
(c) NW Rafter End

(d) SW Rafter End

FIGURE 5-8 Global and Local Hysteresis Curves - 0.80g Peak ELC (ii) Test

5-15
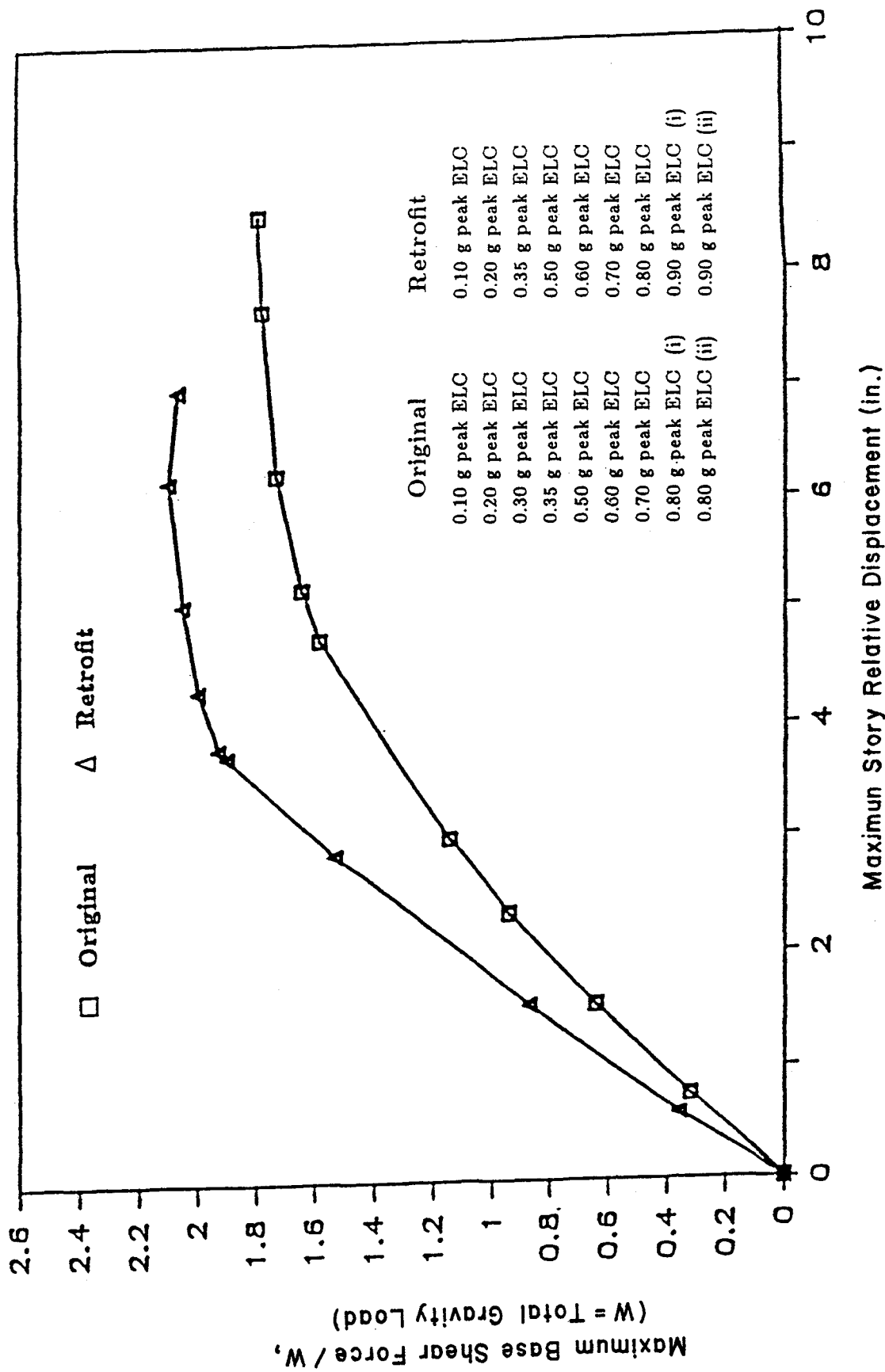
FIGURE 5-9 Experimental Envelopes of Maximum Base Shear vs. Maximum Story Relative Displacement of Original and Retrofitted Test Structures

The chart contains the following legend:

Original	Retrofit
0.10 g peak ELC	0.10 g peak ELC
0.20 g peak ELC	0.20 g peak ELC
0.30 g peak ELC	0.35 g peak ELC
0.35 g peak ELC	0.50 g peak ELC
0.50 g peak ELC	0.60 g peak ELC
0.60 g peak ELC	0.70 g peak ELC
0.70 g peak ELC	0.80 g peak ELC
0.80 g peak ELC (i)	0.90 g peak ELC (i)
0.80 g peak ELC (ii)	0.90 g peak ELC (ii)

□ Original   △ Retrofit

Axis labels:
- Horizontal: Maximun Story Relative Displacement (in.)
- Vertical: Maximum Base Shear Force / W, (W = Total Gravity Load)

—■— : Eccentricity

-○- : Pinned-base

● : Nodal point

FIGURE 5-10(a) Mathematical Model 1
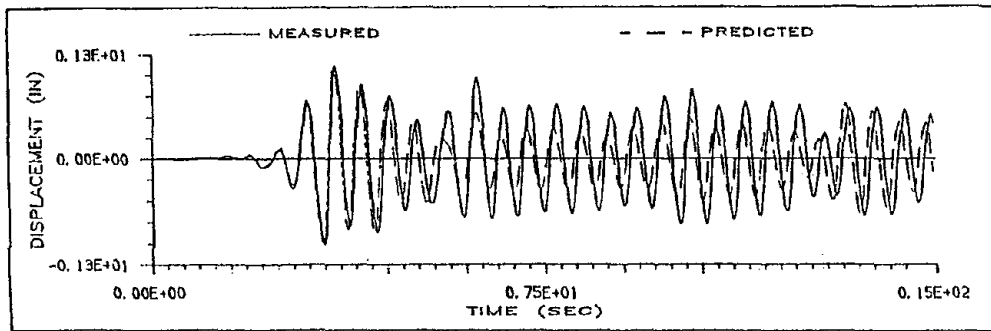
(b.1) Story Relative Displacement
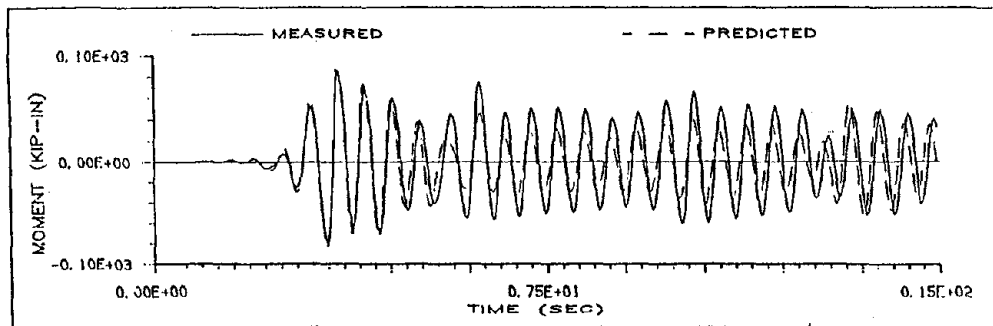
(b.2) Moment at SW Column Top

FIGURE 5-10(b) Analytical Prediction Using Model 1 - 0.15g Peak ELC Test

5-17

━━── : Eccentricity

─O─ : Pinned-base

● : Nodal point

◻ : Dimensionless semi-rigid connection
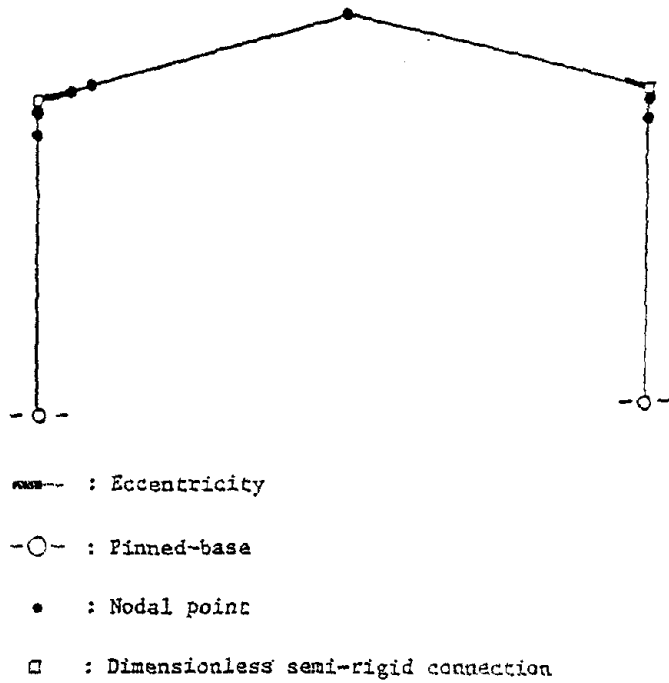
FIGURE 5-10(c) Mathematical Model 2
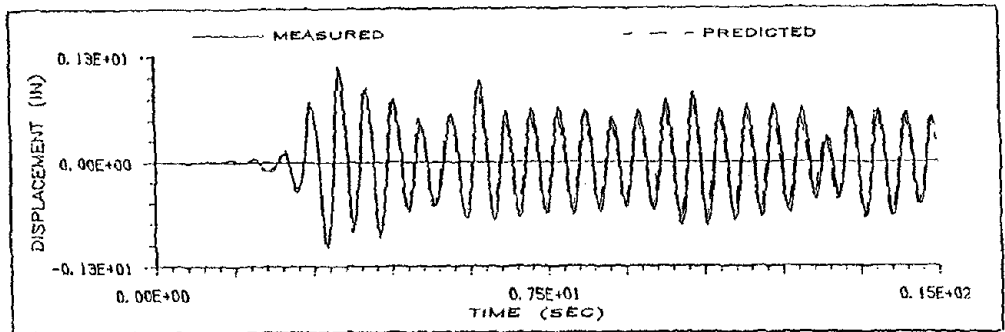
(d.1) Story Relative Displacement
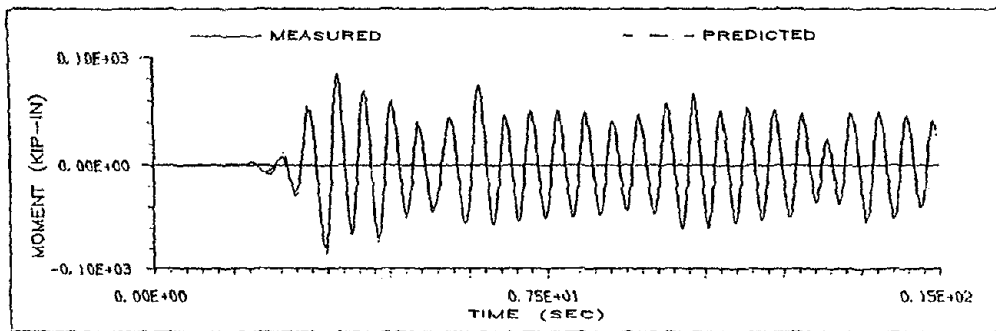
(d.2) Moment at SW Column Top

FIGURE 5-10(d) Analytical Prediction Using Model 2 - 0.15g Peak ELC Test

5-18
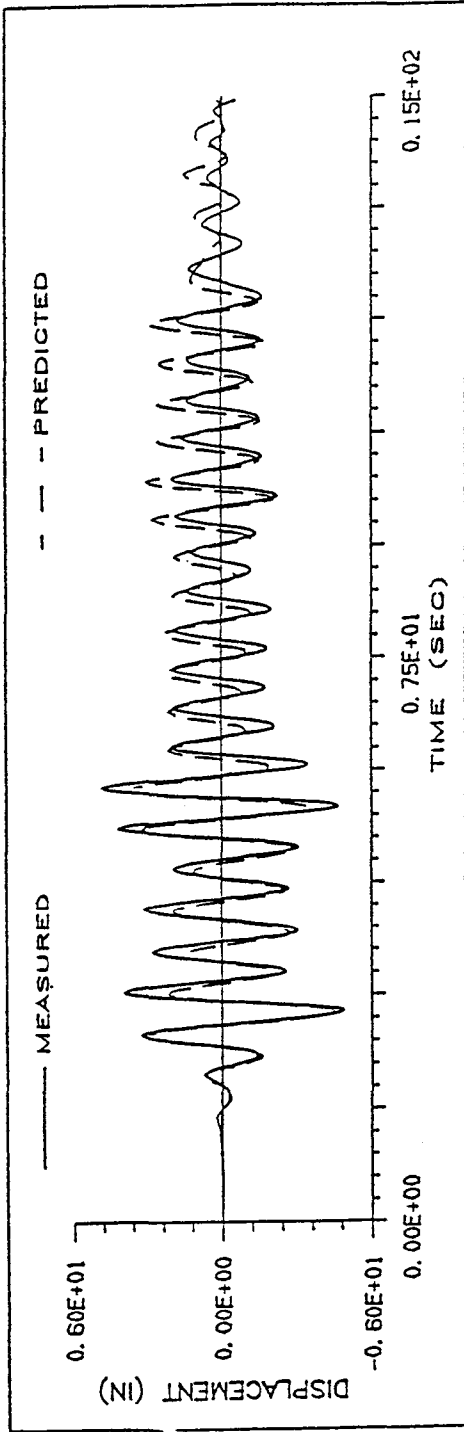
(a) Story Relative Displacement
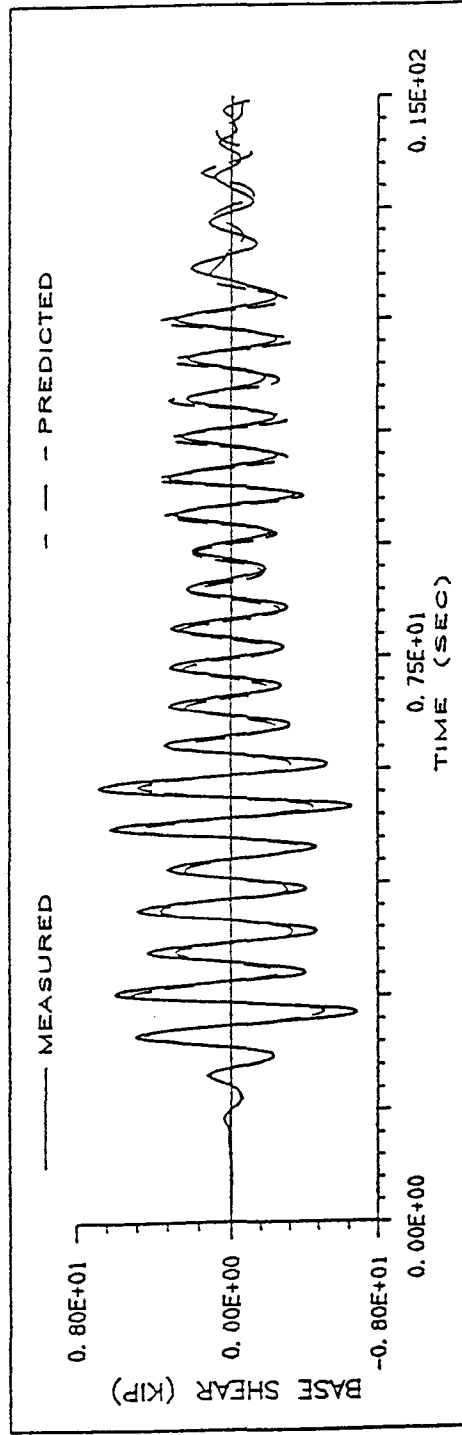
(b) Base Shear Force of West Frame

FIGURE 5-11 Analytical Prediction Using Model 2 - 0.60g Peak ELC Test
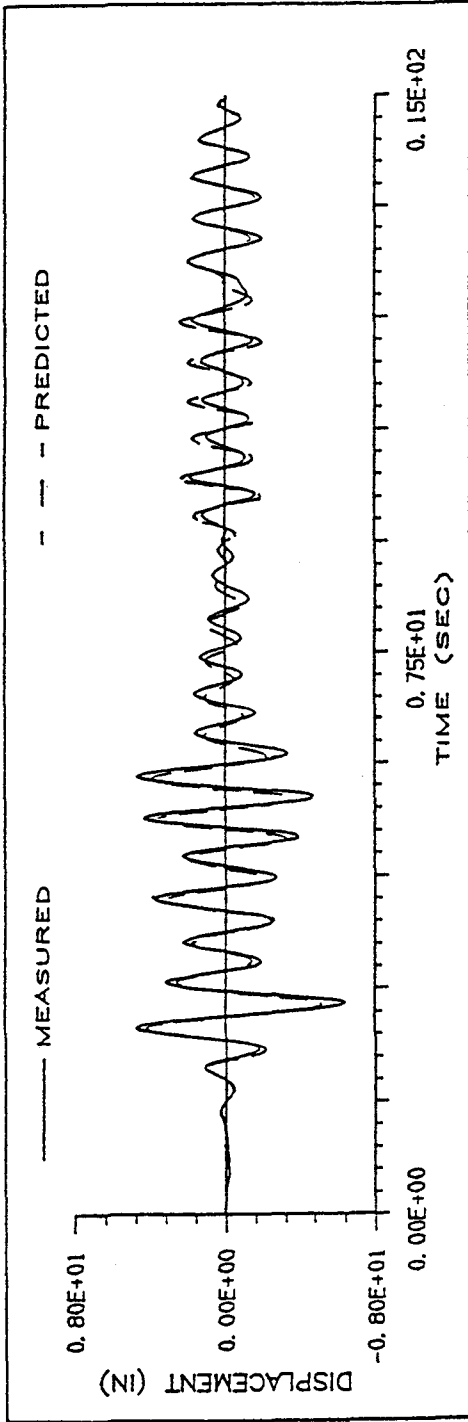
(a) Measured and Predicted Displacement Responses
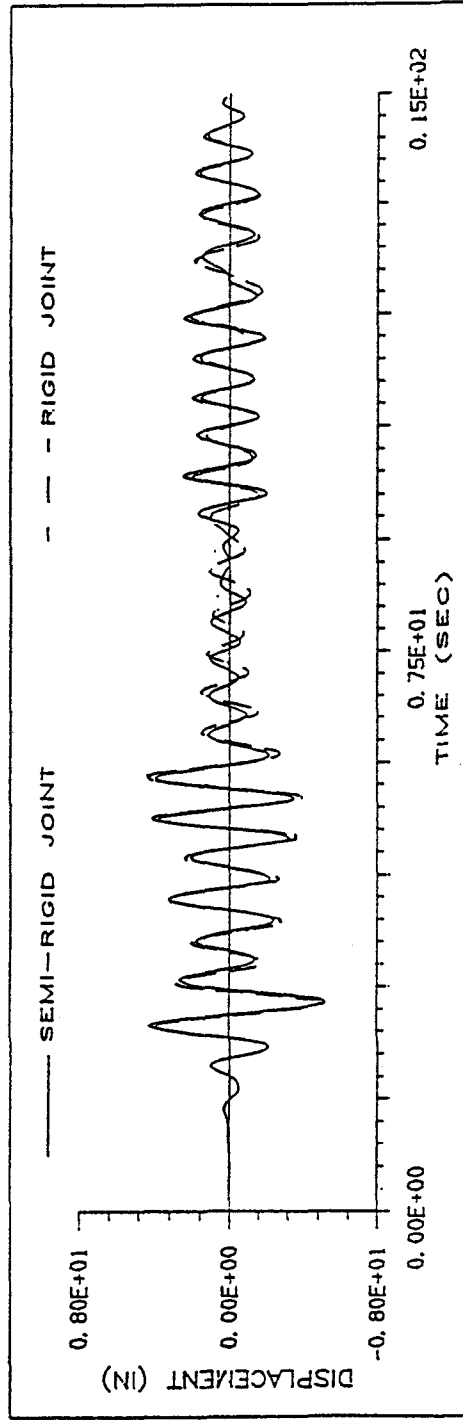
(b) Predicted Displacement Responses—With and Without the Consideration of Semi-rigid Joint

FIGURE 5-12 Analytical Prediction Using Model 2 - 0.80g Peak ELC (ii) Test

5-20

12"

21.5"

SEE DETAIL A
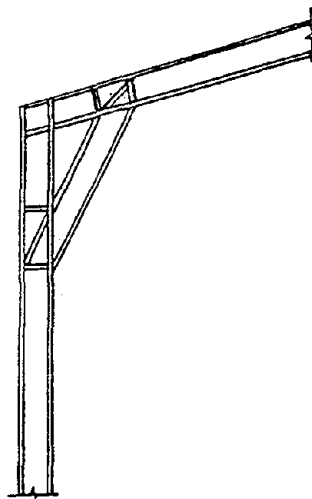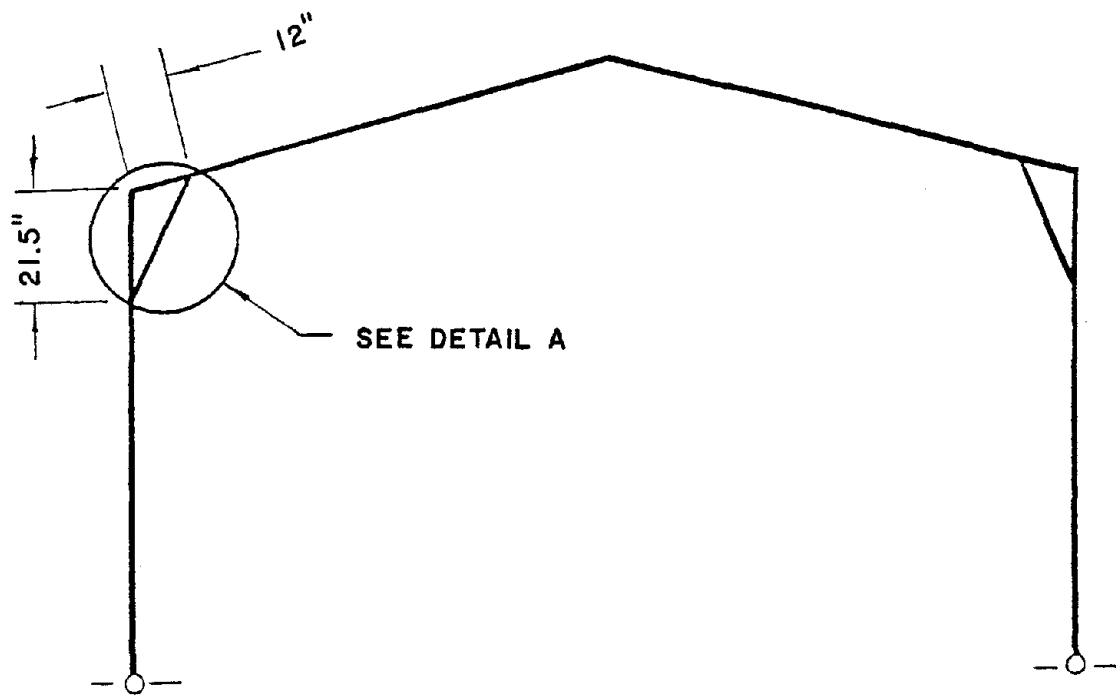
DETAIL A

FIGURE 5-13 Detail of Structural Retrofit With Knee Brace
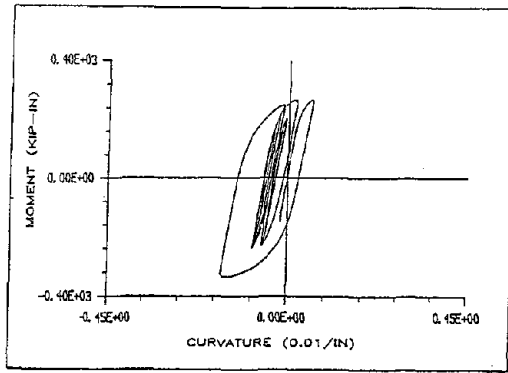
(a) SW Column Top
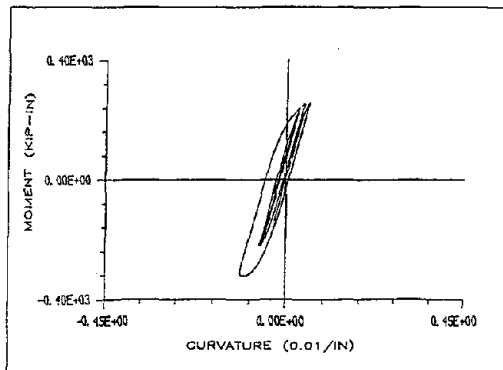
(b) NW Rafter End
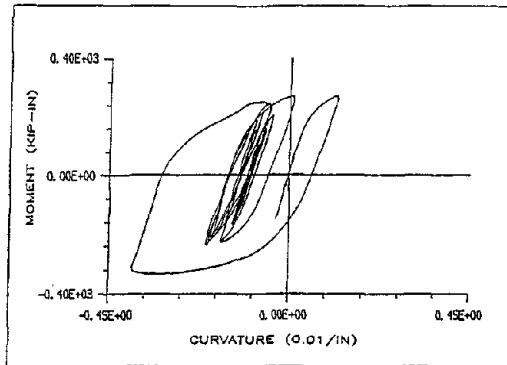
(c) SW Rafter End
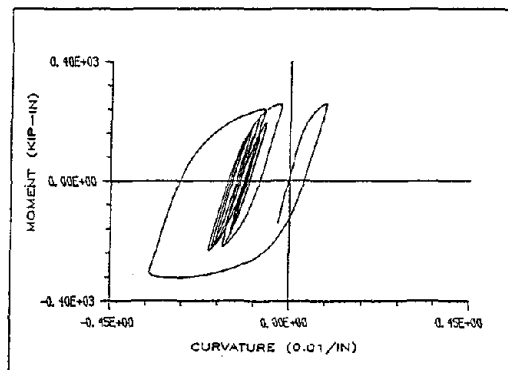
(d) NW Column Top

FIGURE 5-14 Local Hysteresis Curves - 0.90g Peak ELC (ii) Test

5-22
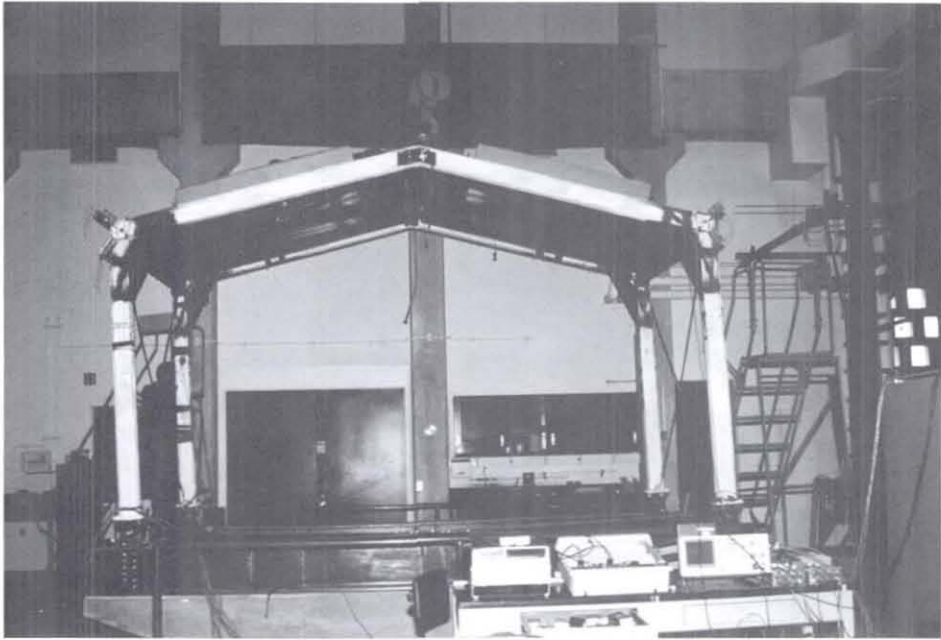
(a) Global Permanent Sidesway
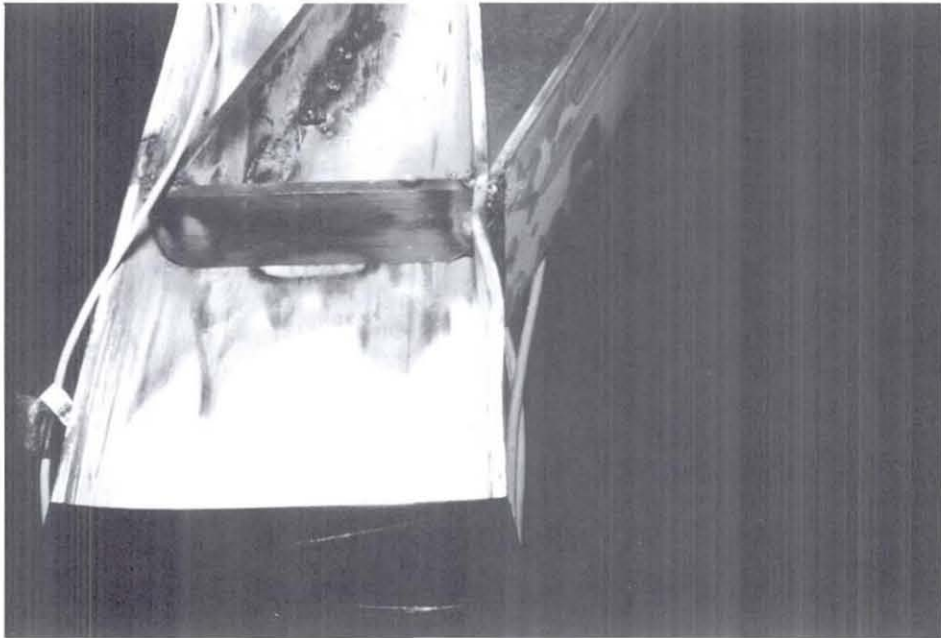
(b) Local Buckling at SW Column Top

FIGURE 5-15 Photographs of Local and Global Damage - 0.90g Peak ELC (ii) Test

SECTION 6

DISCUSSION OF TEST RESULTS

These test results are now reviewed using applicable seismic provisions of UBC and ATC.

6.1 Lumped Mass at Roof Crown

Because of the roof geometry of the gable frame, a lumped mass at the roof ridge in addition to the lumped masses at the column tops was considered necessary. This was intended to account for the larger overturning moment that may be introduced by the mass distributed along the sloping roof. Due to this overturning moment, which is larger than that which would have been observered in a more regular SDOF system, a larger column axial force resulted. A numerical study using mathematical model 2 and the computer program DRAIN-2D was performed to obtain the column axial forces. It was concluded that if $1/2$ of the total mass were lumped at the roof ridge, rather than have it all lumped only at the column tops, there could be an increase of about 12 % in the column axial force under the excitation of the 1940 El Centro earthquake. With such a larger column axial force, the P–Δ effect and the P–M interaction could be larger. (The effect of column axial force on seismic response of a SDOF system is discussed in [15].)

6.2 Story Drift

Another significant test result was that the story drifts of the test structure were much larger than the limits specified by the UBC (0.5 %) and the ATC (1.5 %). It is appreciated that these are specified for fixed-base, regular, shear buildings, and

not for the particular case tested. But no values are given in these model codes for gable structures. As can be seen in Fig. 5–9, the test structure deflects up to 3 % of the story height for the 0.35 g peak ELC test in which only very slight inelastic deformation were observered during the test. In the severe inelastic test, the story drift is up to 7 % of the story height.

6.3 Correlation of Test Results with ATC 3

6.3.1 ATC Provisions

For regular buildings fixed at the base, the design lateral seismic base shear force, V, is to be determined from the following relationship :

$$V \simeq C_S W \tag{1}$$

where

C_S = the seismic design coefficient, and

W = the total gravity load of building

The value of C_S is determined using the formula

$$C_S = \frac{1.2 A_V S}{R T^{2/3}} \tag{2}$$

in which

A_V = the effective peak velocity-related acceleration

S = the coefficient for the soil profile

T = the fundamental period of the building, and

R = the response modification factor

The value of C_S need not exceed $2.5 A_a / R$, where A_a is the the effective peak acceler-

ation. For soil type $S = S_3$, the value of C_S need not exceed $2A_a/R$ when A_a is equal to or greater than 0.3.

Corresponding to the seismic design coefficient, the 5 % damping linear elastic design response spectra specified in the ATC should be reduced by a response modification factor, R, to obtain the base shear force for "significant yield design". While the R values are specified in the ATC for various building types, the determinations of reliable R values are difficult [12,14,16]. The following "facts" concern the response modification factor :

(a)   The response modification factor, R, has been established considering that structures generally have overstrength capacities above the design loads which cause "significant yield".

(b)   The term "significant yield" is not the point where the first yield occurs in any member, but is defined as that level which causes complete plastification of at least the most critical region of the structure.

(c)   The R factor essentially represents the ratio of the forces which would develop under the specified ground motion presuming the structure behaves entirely linearly elastic to the prescribed design forces at the significant yield level.

(d)   Lower values of R should be used for structures which possesses a low degree of structural redundancy. For those structures, all the plastic hinges required for the formation of a mechanism may be formed essentially simultaneously, and at a force level close to the specified design strength. This situation can result in considerably greater P-Δ effects.

(e)   R is an empirical reduction factor intended to account for both the damping and the ductility inherent in the structural system at displacements great enough

to surpass initial yield and approach the ultimate load displacement of the structural system.

According to (d), a lower value of R should be used for the steel gable frame tested since it possesses only one degree of redundancy and the plastic hinges required for the formation of collapse mechanism form essentially simultaneously. However, the actual value to be used is not specified. The R value for the test frame was experimentally determined.

6.3.2 Expected Base Shear Capacities of the Test Structure

Two design methods, the ATC significant yield design and the AISC plastic design, were used to evaluate the base shear capacity of the test frame. The simple model of equivalent lateral forces shown in Fig. 6-1 was assumed. The reactive mass distribution, 1/4 - 1/2 - 1/4, was presumed at the three roof connections. The column axial force was then estimated to be (H/L) $V = 9/16$ V, and the lateral resistant capacity was calculated as follows:

(1) ATC Design Level : In ATC Commentary Chapter 10, a modifier of 1.7 and a capacity reduction factor $\phi = 0.9$ are used to adjust the AISC allowable stresses specified in Section 1.5.1, 1.5.2, 1.5.3 and 1.5.4 to establish the " significant yield" design level. According to this modification and other alterations specified in ATC Chapter 10, the seimsic base shear capacity of the test frame is calculated to be $V = 0.91$ W. (W is the total weight of the reactive mass.) This is shown in Fig. 6-2.

(2) AISC Plastic Design : In AISC Specification Part 2, the design formulas 2.4.1, 2.4.2, 2.4.3 and 2.4.4 are applied to obtain the base shear capacity of the test frame. A load factor of 1.3 specified in Part 2 of AISC Specifications is used. The
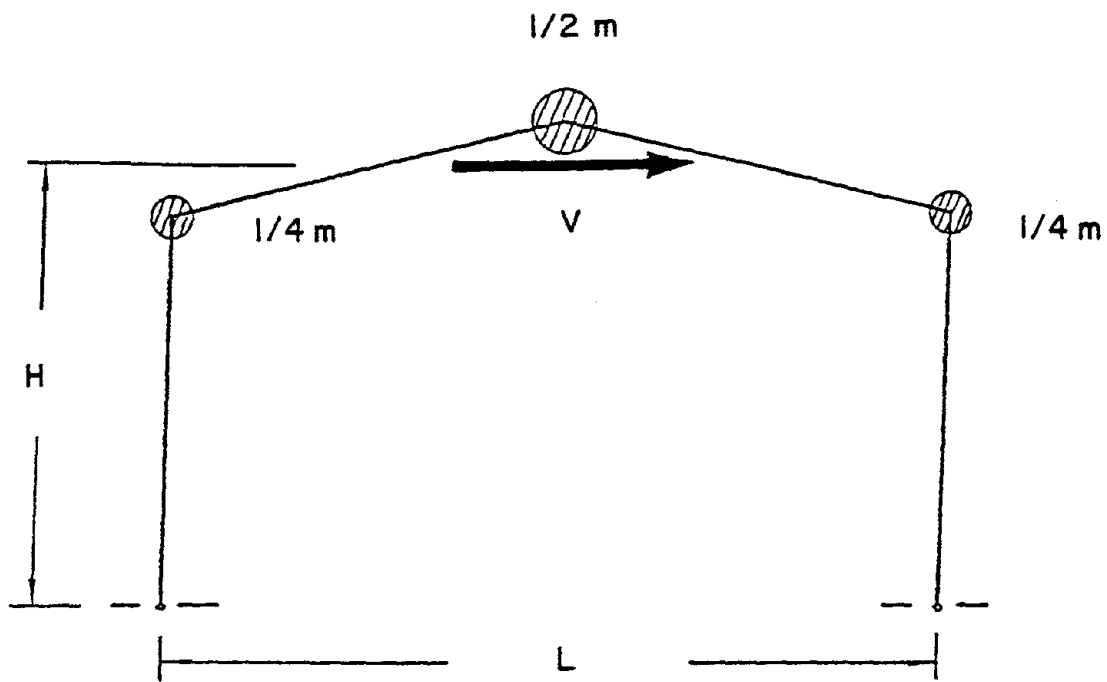
FIGURE 6-1 Assumed Analytical Model for Equivalent Lateral Force

member forces induced by the gravity load are not included in these calculations. The expected lateral shear capacity was calculated to be V = 1.16 W, as shown in Fig. 6–2. It should be noted that the width-thickness ratio of the section W6x9 is slightly larger than that specified in Section 2.7 of AISC Specifications.

In addition, a static, monotonic, analytical prediction was carried out with an assumed elastic-perfectly-plastic moment-curvature model. A yielding moment for the W6x9 of 233.5 kip-in was used. The ultimate strength of this analytical prediction is V = 1.28 W. This, too, is shown in Fig. 6–2.

6.3.3 Discussion of Test Results Related to ATC

The respose modification factors, R, specified in the ATC were determined emperically for various types of structures. The following R values were obtained for the test structure based on the experimental data.

In Fig. 6–2, the 5 % damping linear elastic response spectrum for the 0.8 g ELC acceleration measured at the foundation is shown. The 5 % damping linear elastic response spectrum value corresponding to the experimental structural period range was divided by the predicted structural base shear capacities to establish the R values. For this particular test, the R value, so determined, was 2.10.

It is interesting to note that the experimentally observed ultimate strength of the test structure is very close to the value of the 5 % damping linear elastic response spectrum.

6.4 Discussion of Test Results of Retrofitted Structure

As can been seen from Fig. 5–9, the repaired structure had a considerable amount of increased strength and stiffness. However, the lateral inelastic deforma-
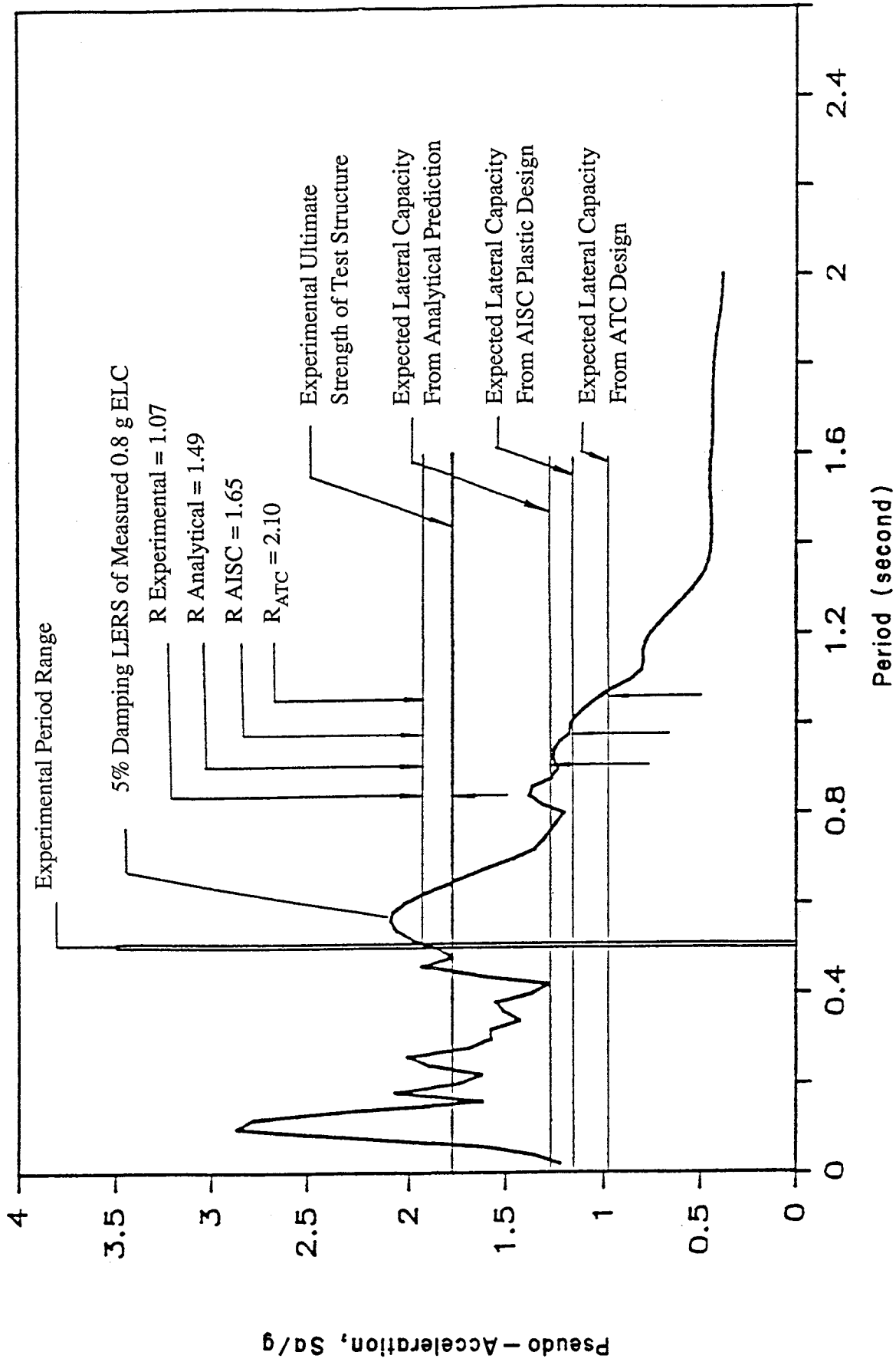
FIGURE 6-2 Experimental Response Modification Factors of Original Test Frame and Base
Shear Capacities Corresponding to Various Methods

tion, when compared against the original structure, slightly decreased.

At the ultimate strength level, the input energy into the retrofitted structure was generally smaller than that of the original structure (see Fig. 6-4). (The input energy was obtained by integrating the time history of base shear force with respect to the time history of ground displacement.) An R value of 1.90 with respect to the ATC design load was obtained for the repaired structure (see Fig. 6-3). This is lower than that of the original structure. The experimental ultimate strength of the retrofitted structure is closer to its elastic response spectrum value than is that of the original structure.
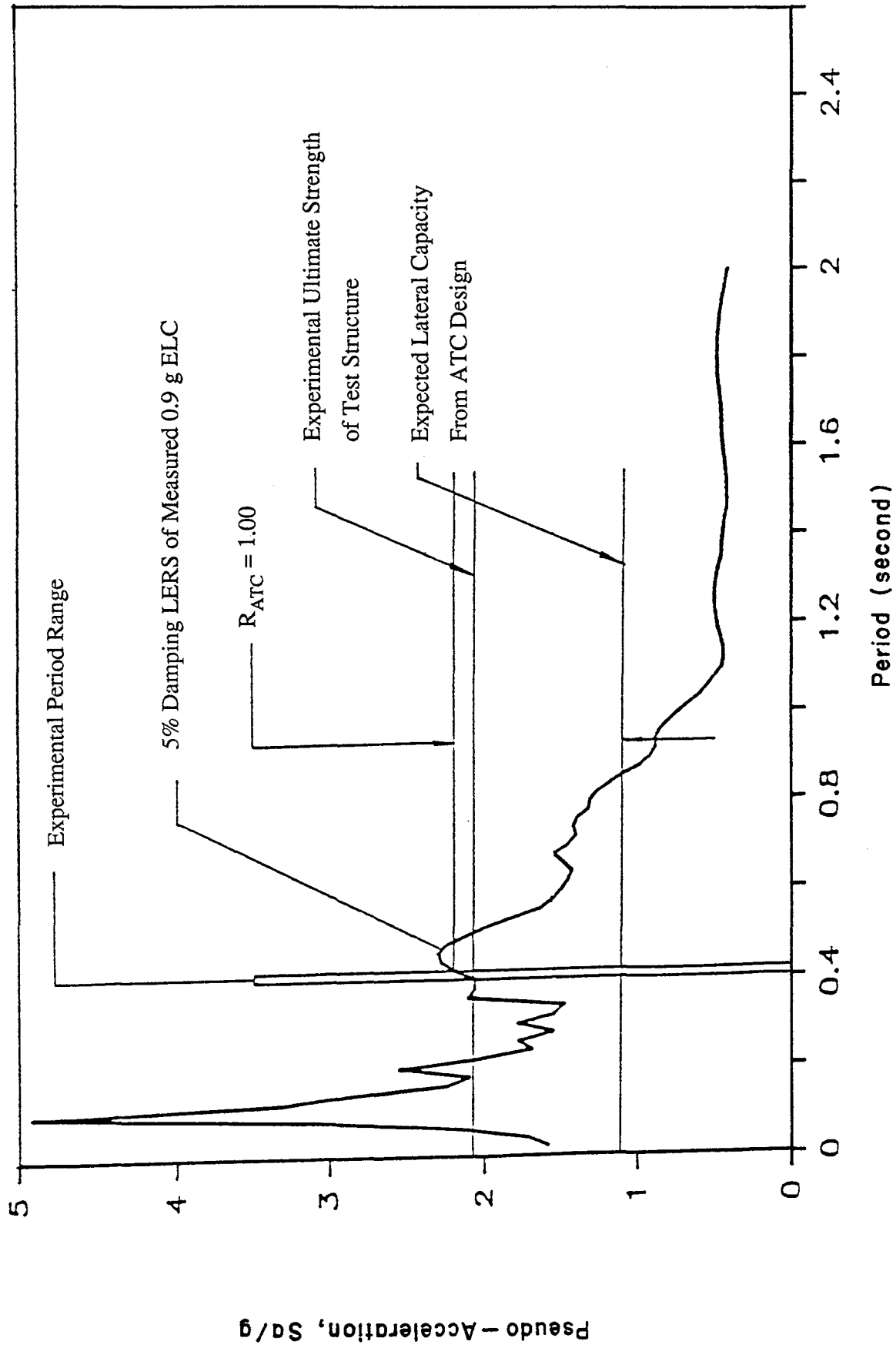
FIGURE 6-3 Response Modification Factor of Retrofitted Test Frame
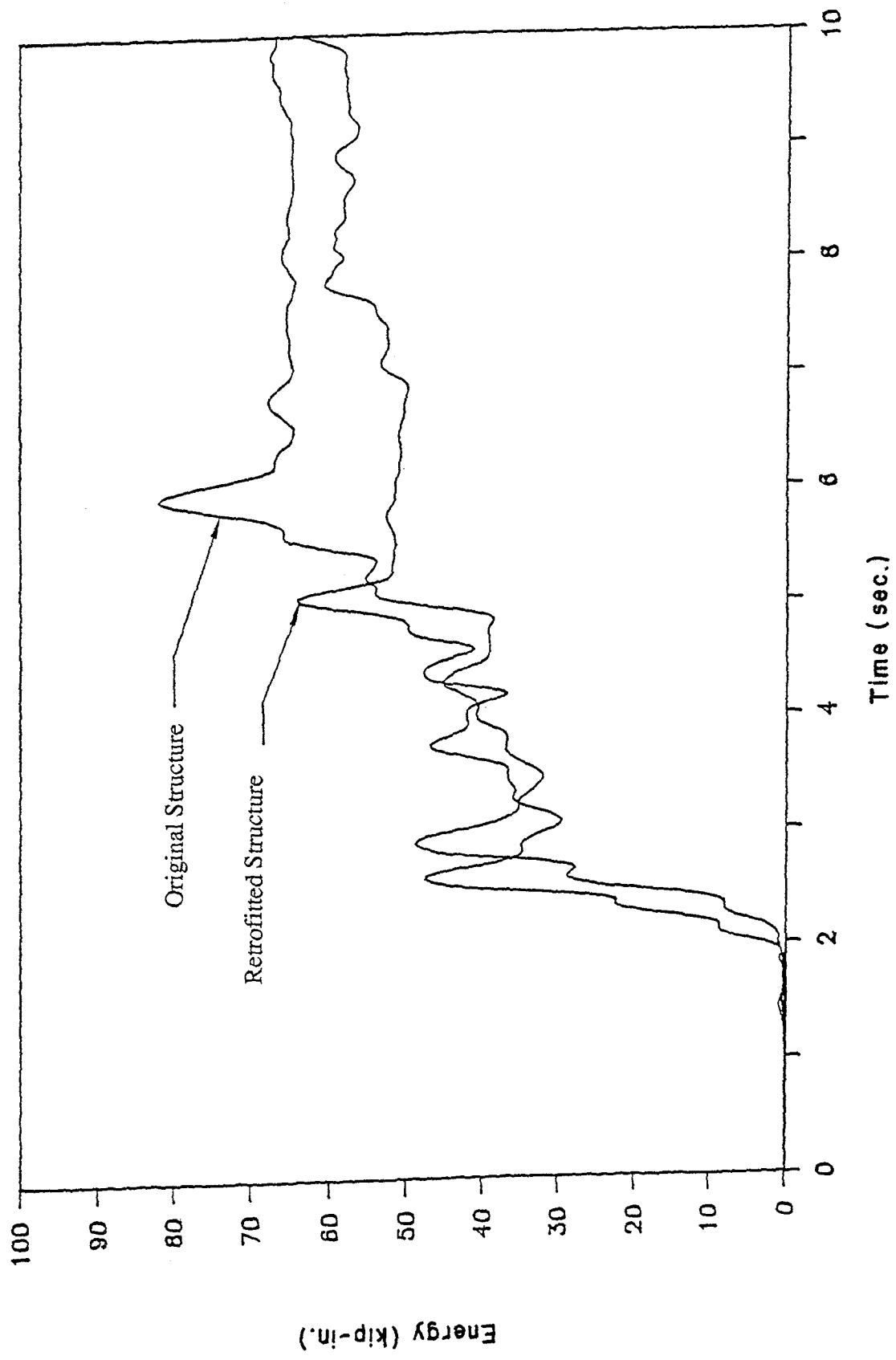
FIGURE 6-4 Comparison of Input Energy to the Retrofitted Test Structure and the Original Test Structure at the Ultimate Strength Test

SECTION 7

OBSERVATIONS AND CONCLUSIONS

Based on experimental observations and analytical predictions, the following conclusions may be drawn :

(1) For the particular test structure and the selected input ground motions used in this experiment, the fidelity of the simulation of ground motion time history was distorted due to the shaking table–test structure interaction at higher excitation levels. This distortion occurred at a few peaks of the acceleration time history. Generally, the distortion was confined in the higher frequency part. (This can be seen by comparing the response spectra of the measured and the input accelerograms.)

(2) Because the distortion in the acceleration time history occurred at a few instants when the test structure experiencing large deformation, the instants of simulation distortion are the instants at which the structure was subjected to severe inelastic deformation (or structural damage).

(3) The envelope curve of the base shear force versus maximum story drift indicated a "transition zone" beyond which the slope of each curve decreased rapidly.

(4) When the lateral ultimate strength was reached, local flange buckling occurred near the column top. There was no perceived local web buckling.

(5) The analytical prediction using DRAIN–2D with the assumed model 2 was found to be generally satisfatory. For this particular gable frame with only one degree of redundancy, and even with reinforced panel zones, the consideration of panel zone deformation is significant for ascertaining the elastic seismic responses of

the structure. Consideration of an additional degree of freedom in the panel zone may not be necessary for the severe inelastic cases where at least two plastic zones form simultaneously.

(6) The story drifts at the moderate and severe damage levels were up to 4 % and 7 %. Strengthening and/or stiffening is necessary if smaller story drifts are desired.

(7) The experimentally determined response modification factor, R, for the test structure was only 2.10 (when compared against the lateral structural capacity determined by ATC significant yield design).

(8) The experimentally observed ultimate lateral strength was very close to the value of 5 % damping linear elastic response spectrum of the measured table acceleration.

(9) For the test structure, the structural retrofit using knee braces was generally feasible and appropriate, and much strength was obtained when compared against that of the original structure. The inelastic story drift of the repaired was reduced by the addition of knee braces. The R value of 1.90 for the retrofitted structure was lower than the R value of 2.10 for the original test structure.

SECTION 8

REFERENCES

1. AISC, "Manual of Steel Construction," 8th Edition, 1980.

2. Lee, G. C., Ketter, R. L. and Hsu, T. L., "Design of Single Story Rigid Frames," Metal Building Manufactured Association, 1981.

3. Meamish, M. J., "Cyclic Loading Tests on Steel Portal Frame Knee Joint," Bulletin of The New Zealand National Society for Earthquake Engineering, Vol. 20, No. 1, March 1987, pp. 42–52.

4. Lee, G. C., Morrell, M. L. and Ketter, R. L.,"Design of Tapered Members," WRC Bulletin, No. 173, june, 1972.

5. Uniform Building Code, 1982 Edition, International Conference of Building Officials, Whittier, California.

6. Applied Technology Council, "Tentative Provisions for the Development of Seismic Regulation for Buildings," U. S. National Bureau of Standards, Special Publication 510, 1978.

7. Ketter, R. L., "The UB Seismic Simulator," Engineering Progress of Western New York, Vol. 3, No. 2, Winter, 1983-84.

8. Hwang, J. S. "An Experimental Study of The Behavior of A Steel Gable Frame Under Strong Earthquake Ground Motions," dissertation submitted to the State University of New York at Buffalo in partial fulfillment of the requirements for the degree of Doctor of Philosophy, January, 1988.

9. Hwang, J. S., Chang, K. C. and Lee, G. C., 'The System Characteristics and Performance of a Shaking Table,' Technical Report NCEER–87–0004, National

Center for Earthquake Engineering Research, June, 1987.

10. Mills, R. S., Kirwinkler, H. and Gere, J. M., "Model Tests on Earthquake Simulator Development and Implementation of Experimental Procedures," Report No. 39, The John A. Blume Earthquake Engineering Center, Stanford University, June, 1979.

11. Mancarz, P. D. and Krawinkler, H., "Theory and Application of Experimental Model Analysis in Earthquake Engineering," Report No. 50, The John A. Blume Earthquake Engineering Center, Stanford University, June, 1981.

12. Bertero, V. V., "Implications of Recent Earthquakes and Research on Earthquake Resistant Design and Construction of Buildings," Report No. EERC 86/03, Earthquake Engineering Research Center, University of California, Berkeley, California, March, 1986.

13. Kannan, A. E. and Powell, G. H., "DRAIN–2D, A General Purpose Computer Program for Dynamic Analysis of Inelastic Plane Structure," Report N0. EERC 73/06 and EERC 73/22, Earthquake Engineering Research Center, University of California, Berkeley, April, 1973 and August, 1975.

14. Uang, C. M. and Bertero, V. V., "Earthquake Simulation Tests and Associated Study of a 0.3–Scale Model of a Six–Story Concentrically Braced Steel Structure," Report No. EERC 86/10, University of California, Berkeley, California, December, 1986.

15. Cheng, F. Y. and Juang, D. S., "The Effects of P-Delta and Semi-Rigid Connections on the Response Behavior of Inelastic Steel Frames Subjected to Cyclic and Seismic Loadings," Stability under Seismic Loadings, ASCE, September, 1986, p. 32–50.

16. Whittaker, A. S., Uang, C. M. and Bertero, V.V., "Earthquake Simulation

Tests and Associated Studies of A 0.3–Scale Model of A Six-Story Eccentrically Braced Steel Structure," Report No. EERC 87/02, University of California, Berkeley, California, July, 1987.

17. Reinhorn, A. M. and Prawel S. P., "Ferrocement in A Large Shaking Table," J. of Structural Engineering, ASCE, Vol. 112, No. 2, Feb., 1986, pp. 401-416.

18. Kaya, I. and McNiven, H. D., "Investigation of The Elastic Characteristics of A Three Story Steel Frame Using System identification," Report No. EERC 78/24, Earthquake Engineering Research Center, University of California, Berkeley, California, Nov., 1978.

19. Valdimarsson, H., Shah, A. H. and McNiven, H. D., "Linear Model to Predict The Nonlinear Seismic Behavior of A One-Story Steel Frame," Report No. EERC 81/13, Earthquake Engineering Research Center, University of california, Berkeley, california, Sep., 1981.

NATIONAL CENTER FOR EARTHQUAKE ENGINEERING RESEARCH
LIST OF PUBLISHED TECHNICAL REPORTS

The National Center for Earthquake Engineering Research (NCEER) publishes technical reports on a variety of subjects related to earthquake engineering written by authors funded through NCEER. These reports are available from both NCEER's Publications Department and the National Technical Information Service (NTIS). Requests for reports should be directed to the Publications Department, National Center for Earthquake Engineering Research, State University of New York at Buffalo, Red Jacket Quadrangle, Buffalo, New York 14261. Reports can also be requested through NTIS, 5285 Port Royal Road, Springfield, Virginia 22161. NTIS accession numbers are shown in parenthesis, if available.

NCEER-87-0001   "First-Year Program in Research, Education and Technology Transfer," 3/5/87, (PB88-134275/AS).

NCEER-87-0002   "Experimental Evaluation of Instantaneous Optimal Algorithms for Structural Control," by R.C. Lin, T.T. Soong and A.M. Reinhorn, 4/20/87, (PB88-134341/AS).

NCEER-87-0003   "Experimentation Using the Earthquake Simulation Facilities at University at Buffalo," by A.M. Reinhorn and R.L. Ketter, to be published.

NCEER-87-0004   "The System Characteristics and Performance of a Shaking Table," by J.S. Hwang, K.C. Chang and G.C. Lee, 6/1/87, (PB88-134259/AS).

NCEER-87-0005   "A Finite Element Formulation for Nonlinear Viscoplastic Material Using a Q Model," by O. Gyebi and G. Dasgupta, 11/2/87, (PB88-213764/AS).

NCEER-87-0006   "Symbolic Manipulation Program (SMP) - Algebraic Codes for Two and Three Dimensional Finite Element Formulations," by X. Lee and G. Dasgupta, 11/9/87, (PB88-219522/AS).

NCEER-87-0007   "Instantaneous Optimal Control Laws for Tall Buildings Under Seismic Excitations," by J.N. Yang, A. Akbarpour and P. Ghaemmaghami, 6/10/87, (PB88-134333/AS).

NCEER-87-0008   "IDARC: Inelastic Damage Analysis of Reinforced Concrete-Frame Shear-Wall Structures," by Y.J. Park, A.M. Reinhorn and S.K. Kunnath, 7/20/87, (PB88-134325/AS).

NCEER-87-0009   "Liquefaction Potential for New York State: A Preliminary Report on Sites in Manhattan and Buffalo," by M. Budhu, V. Vijayakumar, R.F. Giese and L. Baumgras, 8/31/87, (PB88-163704/AS).

NCEER-87-0010   "Vertical and Torsional Vibration of Foundations in Inhomogeneous Media," by A.S. Veletsos and K.W. Dotson, 6/1/87, (PB88-134291/AS).

NCEER-87-0011   "Seismic Probabilistic Risk Assessment and Seismic Margins Studies for Nuclear Power Plants," by Howard H.M. Hwang, 6/15/87, (PB88-134267/AS).

NCEER-87-0012   "Parametric Studies of Frequency Response of Secondary Systems Under Ground-Acceleration Excitations," by Y. Yong and Y.K. Lin, 6/10/87, (PB88-134309/AS).

NCEER-87-0013   "Frequency Response of Secondary Systems Under Seismic Excitation," by J.A. HoLung, J. Cai and Y.K. Lin, 7/31/87, (PB88-134317/AS).

NCEER-87-0014   "Modelling Earthquake Ground Motions in Seismically Active Regions Using Parametric Time Series Methods," G.W. Ellis and A.S. Cakmak, 8/25/87, (PB88-134283/AS).

NCEER-87-0015   "Detection and Assessment of Seismic Structural Damage," by E. DiPasquale and A.S. Cakmak, 8/25/87, (PB88-163712/AS).

NCEER-87-0016   "Pipeline Experiment at Parkfield, California," by J. Isenberg and E. Richardson, 9/15/87, (PB88-163720/AS).

NCEER-87-0017   "Digital Simulation of Seismic Ground Motion," by M. Shinozuka, G. Deodatis and T. Harada, 8/31/87, (PB88-155197/AS).

NCEER-87-0018 "Practical Considerations for Structural Control: System Uncertainty, System Time Delay and Truncation of Small Control Forces," J. Yang and A. Akbarpour, 8/10/87, (PB88-163738/AS).

NCEER-87-0019 "Modal Analysis of Nonclassically Damped Structural Systems Using Canonical Transformation," by J.N. Yang, S. Sarkani and F.X. Long, 9/27/87, (PB88-187851/AS).

NCEER-87-0020 "A Nonstationary Solution in Random Vibration Theory," by J.R. Red-Horse and P.D. Spanos, 11/3/87, (PB88-163746/AS).

NCEER-87-0021 "Horizontal Impedances for Radially Inhomogeneous Viscoelastic Soil Layers," by A.S. Veletsos and K.W. Dotson, 10/15/87, (PB88-150859/AS).

NCEER-87-0022 "Seismic Damage Assessment of Reinforced Concrete Members," by Y.S. Chung, C. Meyer and M. Shinozuka, 10/9/87, (PB88-150867/AS).

NCEER-87-0023 "Active Structural Control in Civil Engineering," by T.T. Soong, 11/11/87, (PB88-187778/AS).

NCEER-87-0024 "Vertical and Torsional Impedances for Radially Inhomogeneous Viscoelastic Soil Layers," by K.W. Dotson and A.S. Veletsos, 12/87, (PB88-187786/AS).

NCEER-87-0025 "Proceedings from the Symposium on Seismic Hazards, Ground Motions, Soil-Liquefaction and Engineering Practice in Eastern North America, October 20-22, 1987, edited by K.H. Jacob, 12/87, (PB88-188115/AS).

NCEER-87-0026 "Report on the Whittier-Narrows, California, Earthquake of October 1, 1987," by J. Pantelic and A. Reinhorn, 11/87, (PB88-187752/AS).

NCEER-87-0027 "Design of a Modular Program for Transient Nonlinear Analysis of Large 3-D Building Structures," by S. Srivastav and J.F. Abel, 12/30/87, (PB88-187950/AS).

NCEER-87-0028 "Second-Year Program in Research, Education and Technology Transfer," 3/8/88, (PB88-219480/AS).

NCEER-88-0001 "Workshop on Seismic Computer Analysis and Design of Buildings With Interactive Graphics," by J.F. Abel and C.H. Conley, 1/18/88, (PB88-187760/AS).

NCEER-88-0002 "Optimal Control of Nonlinear Flexible Structures," J.N. Yang, F.X. Long and D. Wong, 1/22/88, (PB88-213772/AS).

NCEER-88-0003 "Substructuring Techniques in the Time Domain for Primary-Secondary Structural Systems," by G. D. Manolis and G. Juhn, 2/10/88, (PB88-213780/AS).

NCEER-88-0004 "Iterative Seismic Analysis of Primary-Secondary Systems," by A. Singhal, L.D. Lutes and P. Spanos, 2/23/88, (PB88-213798/AS).

NCEER-88-0005 "Stochastic Finite Element Expansion for Random Media," P. D. Spanos and R. Ghanem, 3/14/88, (PB88-213806/AS).

NCEER-88-0006 "Combining Structural Optimization and Structural Control," F. Y. Cheng and C. P. Pantelides, 1/10/88, (PB88-213814/AS).

NCEER-88-0007 "Seismic Performance Assessment of Code-Designed Structures," H.H-M. Hwang, J-W. Jaw and H-J. Shau, 3/20/88, (PB88-219423/AS).

NCEER-88-0008 "Reliability Analysis of Code-Designed Structures Under Natural Hazards," H.H-M. Hwang, H. Ushiba and M. Shinozuka, 2/29/88.

A-2

NCEER-88-0009   "Seismic Fragility Analysis of Shear Wall Structures," J-W Jaw and H.H-M. Hwang, 4/30/88.

NCEER-88-0010   "Base Isolation of a Multi-Story Building Under a Harmonic Ground Motion - A Comparison of Performances of Various Systems," F-G Fan, G. Ahmadi and I.G. Tadjbakhsh, 5/18/88.

NCEER-88-0011   "Seismic Floor Response Spectra for a Combined System by Green's Functions," F.M. Lavelle, L.A. Bergman and P.D. Spanos, 5/1/88.

NCEER-88-0012   "A New Solution Technique for Randomly Excited Hysteretic Structures," G.Q. Cai and Y.K. Lin, 5/16/88.

NCEER-88-0013   "A Study of Radiation Damping and Soil-Structure Interaction Effects in the Centrifuge," K. Weissman, supervised by J.H. Prevost, 5/24/88, to be published.

NCEER-88-0014   "Parameter Identification and Implementation of a Kinematic Plasticity Model for Frictional Soils," J.H. Prevost and D.V. Griffiths, to be published.

NCEER-88-0015   "Two- and Three-Dimensional Dynamic Finite Element Analyses of the Long Valley Dam," D.V. Griffiths and J.H. Prevost, 6/17/88, to be published.

NCEER-88-0016   "Damage Assessment of Reinforced Concrete Structures in Eastern United States," A.M. Reinhorn, M.J. Seidel, S.K. Kunnath and Y.J. Park, 6/15/88, to be published.

NCEER-88-0017   "Dynamic Compliance of Vertically Loaded Strip Foundations in Multilayered Viscoelastic Soils," S. Ahmad and A.S.M. Israil, 6/17/88.

NCEER-88-0018   "An Experimental Study of Seismic Structural Response With Added Viscoelastic Dampers," R.C. Lin, Z. Liang, T.T. Soong and R.H. Zhang, 6/30/88.

NCEER-88-0019   "Experimental Investigation of Primary - Secondary System Interaction," G.D. Manolis, G. Juhn and A.M. Reinhorn, 5/27/88, to be published.

NCEER-88-0020   "A Response Spectrum Approach For Analysis of Nonclassically Damped Structures," J.N. Yang, S. Sarkani and F.X. Long, 4/22/88.

NCEER-88-0021   "Seismic Interaction of Structures and Soils: Stochastic Approach," A.S. Veletsos and A.M. Prasad, 7/21/88, to be published.

NCEER-88-0022   "Identification of the Serviceability Limit State and Detection of Seismic Structural Damage," E. DiPasquale and A.S. Cakmak, 6/15/88, to be published.

NCEER-88-0023   "Multi-Hazard Risk Analysis: Case of a Simple Offshore Structure," B.K. Bhartia and E.H. Vanmarcke, 7/21/88, to be published.

NCEER-88-0024   "Automated Seismic Design of Reinforced Concrete Buildings," Y.S. Chung, C. Meyer and M. Shinozuka, 7/4/88, to be published.

NCEER-88-0025   "Experimental Study of Active Control of MDOF Structures Under Seismic Excitations," L.L. Chung, R.C. Lin, T.T. Soong and A.M. Reinhorn, 7/10/88, to be published.

NCEER-88-0026   "Earthquake Simulation Tests of a Low-Rise Metal Structure," J.S. Hwang, K.C. Chung, G.C. Lee and R.L. Ketter, 8/1/88.